

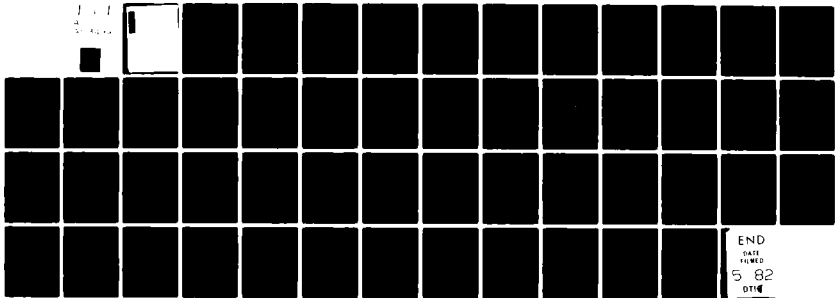
AD-A113 499

NAVAL RESEARCH LAB WASHINGTON DC
F/6 20/9
DRIFT RESISTIVE INTERCHANGE AND TEARING MODES IN CYLINDRICAL GE--ETC(U)
APR 82 J M FINN, W M MANHEIMER, T M ANTONSEN
NRL-MR-4783

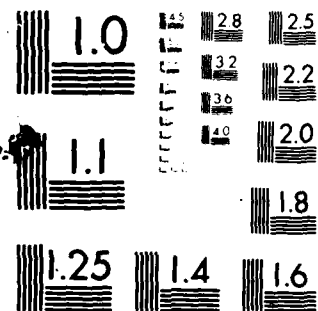
UNCLASSIFIED

NL

1-1-1
1-1-1



END
DATE
FILMED
5 82
DTIC



MICROCOPY RESOLUTION TEST CHART
NATIONAL BUREAU OF STANDARDS-1963-A

AD A113499

SECURITY CLASSIFICATION OF THIS PAGE (When Data Entered)

REPORT DOCUMENTATION PAGE		READ INSTRUCTIONS BEFORE COMPLETING FORM
1. REPORT NUMBER NRL Memorandum Report 4783	2. GOVT ACCESSION NO. AD-A113 499	3. RECIPIENT'S CATALOG NUMBER
4. TITLE (and Subtitle) DRIFT RESISTIVE INTERCHANGE AND TEARING MODES IN CYLINDRICAL GEOMETRY		5. TYPE OF REPORT & PERIOD COVERED Interim report on a continuing NRL problem.
		6. PERFORMING ORG. REPORT NUMBER
7. AUTHOR(s) J.M. Finn, W.M. Manheimer, and T.M. Antonsen, Jr.*		8. CONTRACT OR GRANT NUMBER(s)
9. PERFORMING ORGANIZATION NAME AND ADDRESS Naval Research Laboratory Washington, DC 20375		10. PROGRAM ELEMENT, PROJECT, TASK AREA & WORK UNIT NUMBERS 47-0896-0-1
11. CONTROLLING OFFICE NAME AND ADDRESS Department of Energy Washington, DC 20545		12. REPORT DATE April 13, 1982
		13. NUMBER OF PAGES 51
14. MONITORING AGENCY NAME & ADDRESS (if different from Controlling Office)		15. SECURITY CLASS. (of this report) UNCLASSIFIED
		15a. DECLASSIFICATION/DOWNGRADING SCHEDULE
16. DISTRIBUTION STATEMENT (of this Report) Approved for public release; distribution unlimited.		
17. DISTRIBUTION STATEMENT (of the abstract entered in Block 20, if different from Report)		
18. SUPPLEMENTARY NOTES *Present address: Science Applications, Inc., McLean, VA 22102 This work was supported by the Department of Energy.		
19. KEY WORDS (Continue on reverse side if necessary and identify by block number) Reversed field pinch Resistive interchange instability Hall terms in plasma instability		
20. ABSTRACT (Continue on reverse side if necessary and identify by block number) Resistive interchange and tearing modes are studied including the effects of electron parallel pressure gradient and ion polarization drift (Hall terms) as well as finite plasma compressibility and perpendicular resistivity. It is found that for unfavorable curvature and weak tearing forces (positive but small Δ') all modes are stabilized provided the effects of the Hall (drift) terms are large enough. The principal stabilizing influences are plasma compression and coupling to outgoing drift waves. The relevance to reversed field pinch and spheromak experiments is discussed.		

DD FORM 1473
1 JAN 73EDITION OF 1 NOV 65 IS OBSOLETE
S/N 0102-014-6601

SECURITY CLASSIFICATION OF THIS PAGE (When Data Entered)

DTIC
ELECTE
APR 15 1982

CONTENTS

I. INTRODUCTION	1
II. THE EQUATIONS AND SCALINGS	5
III. APPROXIMATE ANALYTIC SOLUTIONS	12
IV. NUMERICAL RESULTS	25
V. CONCLUSIONS	39
ACKNOWLEDGMENTS	40
REFERENCES	41
APPENDIX	43



Accession For	
DTIC	OTHER
DTIC	OTHER
used	
action	
By	
Distribution/	
Confidentiality Codes	
Date	
A	

DRIFT RESISTIVE INTERCHANGE AND TEARING MODES IN CYLINDRICAL GEOMETRY

I. Introduction

In a plasma with unfavorable average curvature along each field line, it has long been appreciated¹⁻³ that finite conductivity weakens the shear stabilization criterion of ideal interchange modes (the Suydam criterion⁴ or its toroidal generalization, the Mercier criterion).^{5,6} In a sheared slab with density gradient and with gravity simulating curvature, and with incompressible displacements, the plasma is unstable to an infinite number of such resistive interchange (or resistive g) modes localized near each mode rational surface (at which $\underline{k} \cdot \underline{B} = 0$, where \underline{k} is the wave vector).

In a cylindrical model with curvature and pressure gradient these results are strongly modified by plasma compression.³ In a plasma with very low pressure (but finite pressure gradient) the results are formally identical to those in the slab model. Finite plasma pressure introduces the stabilizing effect of plasma compression which, if large enough, stabilizes all but one mode for each mode rational surface. This mode, whose magnetic perturbation is not totally localized to the mode rational surface, and which couples to the exterior (magnetohydrodynamic) region, is in fact the tearing mode. For unfavorable curvature and stabilizing tearing forces from the outer region ($\Delta' < 0$, defined in Sec. III), it is driven unstable by curvature in the same manner as the localized resistive interchanges. It has recently been pointed out⁷ that for large $|\Delta'|$ or small D , the tearing-like coupling to the exterior region has a strong stabilizing influence that reduces the growth rate from the conventional $D^{2/3}$ scaling (D is the Suydam parameter, defined in Sec. III) to a D^4/Δ'^4 scaling. This transition has also been observed in numerical simulations.⁸

It has been suggested that resistive interchange modes are responsible for transport in reversed field pinches,⁹ which have unfavorable average curvature

because their safety factor q (defined in Sec. II) is less than unity. It is also possible that fluctuations¹⁰ which are seen late in the discharge in the Los Alamos experiment (ZT-40) and which are predominately $m = 0$ (m is the poloidal mode number), are resistive interchange modes. The transition from $D^{2/3}$ behavior to D^4/Δ^4 behavior in reversed field pinch geometry occurs at $\beta \sim 7\%$ for magnetic Reynolds number $R_m = 10^3$ but at $\beta \sim 1\%$ for $R_m = 10^6$, so that present day devices (with $\beta \sim 10\%$) should be in the larger growth rate (i.e. $D^{2/3}$) regime. We shall discuss this point further in Sec. IV.

In addition, compact torus devices such as the spheromak, which have $q < 1$, and which therefore have unfavorable average curvature, should be subject to such instabilities. It has been recently found that spheromaks are optimally stable to ideal magnetohydrodynamic tilt and shift modes if their flux surfaces near the magnetic axis are nearly circular.^{11,12} Also, transport studies indicate that the toroidal current and temperature become quite peaked near the magnetic axis, as in a tokamak.¹³ Therefore, in spite of the small toroidal aspect ratio of spheromaks, which may cause resistive instabilities to have some ballooning like structure (i.e. to be sensitive to local as well as average curvature), the variation of the field line curvature along field lines in the region of large pressure gradient may be small.

The purpose of the present paper is to investigate the drift, or Hall effects, on these instabilities. These terms become important in the component of Ohm's law parallel to the magnetic field when $|\omega| < |\omega_{*e}|$ (ω_{*e} is the electron diamagnetic frequency kcT_e/eBL_n , and L_n is the density gradient scale length) and represents the fact that a parallel component of the electric field may be balanced by parallel electron pressure gradient as well as collisions. The inclusion of these terms in the perpendicular component of Ohm's law is equivalent to the inclusion of the ion polarization drift. As we shall see, the

effect of the inclusion of the Hall terms on these modes is to impart a real part to their frequency $\omega_r \lesssim \omega_{*e}$ and, if these effects are strong enough, to stabilize the modes altogether. The $m = 0$ fluctuations in ZT-40 have a frequency which is of order ω_{*e}^{10} .

The model we use has cylindrical geometry, and thus has field line curvature rather than a fictitious gravity. The only toroidal effect is that the axial wave number is quantized $k = k_z = -n/R$, where R is the major radius. We include finite plasma compressibility (with electrons isothermal along field lines and adiabatic ions) and perpendicular resistivity, which is neglected in tokamak ordering.

In Sec. II we explain the physical model in more detail and derive the basic equations.

In Sec. III we derive analytic results in several limiting cases, including the incompressible "slab" limit ($p \rightarrow 0$, $dp/dr \neq 0$) where plasma compression and perpendicular resistivity are ignored. We recover the dispersion relation for the drift tearing mode^{14,15} from a more general dispersion relation for drift-tearing-resistive interchange modes. This more general result shows that slab-like resistive interchange modes remain unstable for arbitrarily large ω_{*e}/Q_r , where Q_r is a nominal resistive instability growth rate (defined in Sec. II) but with a growth rate that scales as $\omega_{*e}^{-1/2}$. We also derive a dispersion relation with perpendicular resistivity and plasma compression for localized modes with ω_{*e} large; this result shows that for large ω_{*e} no such mode is unstable. In the Appendix we generalize this to less localized modes which couple to the outer region through outward propagating drift waves and show that no instability exists for large ω_{*e}/Q_r unless Δ' (defined in Sec. III) is above a critical value which is positive. It is possible that the fluctuations seen in reversed field pinches are resistive interchange modes which become unstable when the mode

rational surface is near the edge of the plasma, where compressional stabilization is at a minimum.

In Sec. IV we show numerical results which are consistent with the analytic results of Sec. III in showing that no instability exists for large enough ω_{*e}/Q_r , when the coupling to outward propagating drift waves is strong. We find the critical values for ω_{*e} for the localized and nonlocalized (tearing) mode and find these values below but very near typical values for reversed field pinch parameters.

II. The Equations and Scalings

In this section we review the derivation of the equations for resistive interchange modes including the additional effect of the Hall term in Ohm's law. As we will see, these terms allow for the coupling of resistive interchange modes to drift modes. Since it is now known that drift waves are stable in slab geometry in a sheared field,¹⁶ this coupling is a stabilizing effect.

We adopt the scaling as assumed in Coppi, Greene and Johnson³ and our previous work.⁷ Outside a small distance L_r away from the rational surface, the ideal MHD equations hold, but within this distance L_r , finite resistivity, perpendicular inertia, and Hall effects (electron pressure gradient and polarization drift) are important. We will assume that $L_r/a \sim \epsilon$, where a is the radius of the mode rational surface and a is also assumed to be roughly equal to the scale of variation of the eigenfunction in the other direction perpendicular to \underline{B} . Since the plasma is assumed to be stable to localized ideal magnetohydrodynamic modes (Suydam stable), the growth rate also scales as ϵ . In this, the so-called slow interchange ordering of Ref. 3, ϵ also scales as $\eta^{1/3}$.

In cylindrical geometry, the eigenfunction has the form $\tilde{f}(r) \exp(\gamma t + im\theta + ikz)$ where, in a large aspect ratio torus, $k = -n/R$. A superscript \sim denotes a perturbed quantity. The mode rational surface is determined by

$$m = nq, \quad (1)$$

where $q = rB_z/RB_\theta$. The operator $\underline{B} \cdot \underline{\nabla}$ operating on a scalar is given by

$$\underline{B} \cdot \underline{\nabla} \rightarrow - \frac{inB_\theta q}{a} (r - a) + O(r - a)^2 \quad (2)$$

where $r = a$ is the location of the mode rational surface; within the singular region the right hand side of (2) is of order ϵ . (We use this form rather than

that of Ref. 3 since it applies also to $m = 0$ modes, which have their rational surface where $B_z = 0$.)

Since the resistive interchange mode is characterized by nonzero resistivity allowing the fluid to slip through the sheared field near the rational surface, the mode is mostly fluid flow with only a small magnetic perturbation.

Thus $\underline{\tilde{B}} \sim \epsilon \underline{\xi}$ where $\underline{\xi}$ is the linearized fluid displacement. Since the growth rate is assumed to be slow compared to the magnetosonic speed, we have

$$\underline{B} \cdot \underline{\tilde{B}} + \tilde{p} = 0. \quad (3)$$

where \tilde{p} is the perturbed total (electron plus ion) pressure. However, for Ohm's law, we use the full ion momentum equation

$$\underline{E} + \underline{v} \times \underline{B} - \eta \underline{J} = \frac{M}{e} \frac{\partial \underline{v}}{\partial t} + M \underline{\nabla} p_i / \rho e, \quad (4)$$

where p_i is the ion pressure, ρ is the density and M is the ion mass. We assume that the ions obey an adiabatic equation of state, i.e. the perturbed ion pressure, \tilde{p}_i is given by

$$\tilde{p}_i = -p_i' \xi_r - \Gamma p_i (\underline{\nabla} \cdot \underline{\xi}), \quad (5)$$

where Γ is the specific heat ratio and $\underline{\xi}$ is the fluid displacement. Since both terms on the right hand side of Eq. (5) contribute roughly equally to the perturbed ion pressure, $\underline{\nabla} \cdot \underline{\xi}$ is of order ϵ .

The electrons, on the other hand, are assumed to be isothermal along a field line, or

$$\underline{B} \cdot \underline{\nabla} \tilde{T}_e + \underline{\tilde{B}} \cdot \underline{\nabla} T_e = 0,$$

which gives

$$\hat{T}_e = \frac{a \hat{B}_r}{\ln B_\theta q x} T_e', \quad (6)$$

where henceforth $x = r - a$ and the perturbed electron pressure is $\hat{p}_e = (\rho \hat{T}_e + \tilde{\rho} T_e')/M$. Note that if \hat{B}_r has even symmetry about the field line, \hat{T}_e is singular. This singularity can be removed by accounting for finite electron thermal conduction along a field line. However if \hat{B}_r has odd symmetry, or if $T_e' = 0$ at $r = a$, there is no singularity. If we define a local coordinate system $\underline{i}_r, \underline{i}_\parallel$ and $\underline{i}_\perp = \underline{i}_r \times \underline{i}_\parallel$, where \underline{i}_r and \underline{i}_\parallel are unit vectors in the direction of \underline{r} and \underline{B} , then

$$\underline{\xi} = \xi_r \underline{i}_r + \xi_\parallel \underline{i}_\parallel + \xi_\perp \underline{i}_\perp,$$

$$\underline{\hat{B}} = \hat{B}_r \underline{i}_r + \hat{B}_\parallel \underline{i}_\parallel + \hat{B}_\perp \underline{i}_\perp,$$

where $\xi_{\parallel\perp} \sim \epsilon^0$, $\xi_r, \hat{B}_{\perp\parallel} \sim \epsilon$ and $\hat{B}_r \sim \epsilon^2$. Then the condition that $\underline{\nabla} \cdot \underline{\xi} = 0$ to lowest order, $\underline{\nabla} \cdot \underline{\hat{B}} = 0$, pressure balance and the continuity equation gives the following four equations

$$\xi_\perp + \frac{1RB_\theta}{nB} \frac{\partial \xi_r}{\partial r} = 0, \quad (7)$$

$$\hat{B}_\perp + \frac{1RB_\theta}{nB} \frac{\partial \hat{B}_r}{\partial r} = 0, \quad (8)$$

$$\hat{B}\hat{B}_\parallel = p_i' \xi_r + \Gamma p_i (\underline{\nabla} \cdot \underline{\xi}) - \tilde{\rho} T_e'/M - \frac{a \hat{B}_{re}}{\ln B_\theta q x M} T_e', \quad (9)$$

$$\hat{\rho} = -\xi_r \rho' - \rho (\underline{\nabla} \cdot \underline{\xi}). \quad (10)$$

Two other equations, which are the same as in Ref. 3, come from operating on the total momentum equation with $\underline{B} \cdot$ and with either $\underline{\nabla} \cdot (B^{-2} \underline{B} \times)$ or $\underline{B} \cdot \underline{\nabla} \times$ are

$$\rho \gamma^2 B \xi_{\parallel} = - (p_e + p_i) \hat{B}_r - \frac{inB_{\theta} q \hat{B}_x}{a} - \hat{B}_{\parallel}. \quad (11)$$

$$\rho \gamma^2 \frac{d^2 \xi_r}{dr^2} = \frac{2n^2 B}{R^2 a} \hat{B}_{\parallel} - \frac{inB_{\theta} q \hat{B}_x}{a} \frac{d^2 \hat{B}_r}{dr^2}. \quad (12)$$

Equation (12) is called the annihilated momentum equation, since the operator annihilates information about propagation along the lines of force and also information about $\nabla(\underline{B} \cdot \underline{\hat{B}} + \hat{p})$. In order to neglect collisional and collisionless ion viscosity in Eq. (12), we require $T_i \ll T_e$. The next two equations are the radial and parallel components of Ohm's law. It is these two equations that contain the effects of the additional Hall terms. They are

$$\hat{B}_r - \frac{\eta}{\gamma} \frac{d^2 \hat{B}_r}{dr^2} = - \frac{inB_{\theta} q \hat{x}}{a} \xi_r - \frac{M}{e} \gamma \frac{inB}{R_{\theta} B} \xi_{\parallel}, \quad (13)$$

$$\begin{aligned} \hat{B}_{\parallel} - \frac{\eta}{\gamma} \frac{d^2 \hat{B}_{\parallel}}{dr^2} &= \frac{-inB_{\theta} q \hat{x}}{a} \xi_{\parallel} - B(\underline{\nabla} \cdot \underline{\xi}) - \frac{(p + B^2)}{B} \hat{\xi}_r, \\ &+ \frac{M\gamma}{e} \frac{\partial \xi_{\perp}}{\partial r} + \frac{M}{\rho^2 e} \frac{inB}{B_{\theta} R \gamma} (\hat{p}_i \frac{dp}{dr} - \hat{p} \frac{dp_i}{dr}). \end{aligned} \quad (14)$$

As in Ref. 3 the eight equations, (7) - (14), can be reduced to three second order differential equations for the three variables \hat{B}_r , \hat{B}_{\parallel} and ξ_r . We introduce the variables used in Ref. 3: $Q = \gamma/Q_r$, $\xi = \xi_r$, $X = x/L_r$, and

$$\psi \equiv \frac{-ia}{nB_{\theta} q L_r} \hat{B}_r,$$

$$T = \frac{-2Ba}{R^2 q^2 B_{\theta}^2} \hat{B}_{\parallel},$$

$$D = - \frac{2p' a}{B_{\theta}^2 R^2 q'^2},$$

$$\beta = 2p(a)/B^2,$$

$$S = 4/R^2 q'^2,$$

$$L_r = \left(\frac{\rho \eta^2 a^2}{n^2 B_{\theta}^2 q'^2} \right)^{1/6},$$

$$Q_r = \left(\frac{\eta n^2 B_{\theta}^2 q'^2}{\rho a^2} \right)^{1/3},$$

as well as two new variables g (to measure the strength of the Hall effect)

$$g = \frac{R_m^{1/3} |nq' a|^{1/3}}{|Rq'|} \left(\frac{V_A}{\omega_{ci} a} \right), \quad (15)$$

where ω_{ci} is the ion cyclotron frequency using B_{θ} , R_m is the magnetic Reynolds number, $R_m = \frac{aV_A}{\eta}$, V_A is the Alfvén speed using B_{θ} , and $\kappa = (1 - \Gamma p_1 \rho' / p_1' \rho)(p_1' / p')$. In terms of these variables the three coupled second order equations reduce to

$$\frac{d^2 \xi}{dx^2} = \frac{1}{Q^2} x \frac{d^2 \psi}{dx^2} - \frac{1}{Q^2} T, \quad (16)$$

$$\frac{d^2 \psi}{dx^2} = Q(\psi + x \xi) + 1Q_* \psi + \frac{21gT}{S} x, \quad (17)$$

$$\frac{d^2 T}{dX^2} = Q \left(1 + \frac{X^2}{Q^2} + \frac{2}{\Gamma_c \beta} \right) T + Q \left(S - D - \frac{2D}{\Gamma_c \beta} \right) \xi + \frac{D}{Q} X \psi + i Q_* \frac{2}{\Gamma_c \beta} \kappa (T - D\xi) - 2i Q^2 g \frac{d^2 \xi}{dX^2}, \quad (18)$$

where $Q_* = 2gD/S$.

In deriving Eqs. (16) - (18), we have further assumed that $\nabla T_e = 0$ so that subtleties concerning singular behavior of electron temperature are avoided. The Γ_c in Eq. (18) is then a combined specific heat ratio which accounts for the fact that the electrons are isothermal but the ions are adiabatic,

$$\Gamma_c = \frac{\rho T_e / M + \Gamma p_i}{p_e + p_i}. \quad (19)$$

If the ion temperature is zero, $\Gamma_c = 1$.

The terms in Eqs. (17) and (18) which contain the g factor are the effects of the Hall terms. Since they are all purely imaginary, they provide a real part of the frequency. Notice that the terms in Eq. (18) proportional to κ are zero for a "baroclinic" ion pressure profile, that is

$$\frac{1}{\rho} \frac{d\rho}{dx} - \frac{1}{\Gamma p_i} \frac{dp_i}{dx} = 0 \quad (20)$$

or $p_i \sim \rho^\Gamma$. In our numerical computations, we generally make this assumption. Also, we have neglected collisionless and collisional ion viscosity and thermal conduction. For reversed field pinch parameters, this can only be justified if $T_e \gg T_i$. Finally, to make contact with conventional drift waves and drift ordering, let us note that the drift wave frequency, $mcT_e \rho' / eBap$ is given by

$$\omega_{*e} = Q_* Q_r. \quad (21)$$

As we will see in the next section, combinations like $Q + iQ_*$ (proportional to $\omega - \omega_{*e}$) frequently appear in the analysis of Eqs. (16) - (18) and it is through these terms that resistive interchange and tearing modes couple to stable drift waves.

III. Approximate Analytic Solutions

There are at least three limits in which one can get analytic solutions to Eqs. (16) - (18). The first is $g = 0$ and these have been discussed fully in Refs. 1 - 3, 7. The second is the unphysical, yet illuminating, limit $\Gamma_c \rightarrow 0$ and the third is the limit $T_i = 0$, $g^3 \beta \gg 1$.

We begin by discussing the limit $\Gamma_c \rightarrow 0$. In this limit, plasma compression makes no contribution to perturbed pressure. In this sense, it is rather like the incompressible theory of resistive interchange modes in a slab, where the curvature - pressure gradient term in Eq. (12) (proportional to \tilde{E}_\parallel) is replaced by a gravity - perturbed density term. As we shall see, the results of this limiting case are similar to the simple slab mode without Hall terms, in the sense that an unstable mode exists for arbitrarily large shear and g . If $\Gamma_c = 0$, then Eq. (18) shows that $T = D \xi$, so that Eqs. (17) and (16) become, respectively

$$\frac{d^2 \Psi}{dX^2} = (Q + iQ_*) (\Psi + X \xi) \quad (22)$$

$$\frac{d^2 \xi}{dX^2} = \frac{X^2}{Q^2} (Q + iQ_*) \xi - \frac{D}{Q^2} \xi + \frac{X}{Q^2} (Q + iQ_*) \Psi \quad (23)$$

where we have used Eq. (22) to eliminate the $d^2 \Psi/dX^2$ term in Eq. (16). To solve Eqs. (22) and (23) we first make the constant Ψ approximation. If ξ is even in X , Ψ is odd, so that with this approximation $\Psi = 0$. In this case the lowest order eigenfunction ξ is given by $\xi = \exp(-\sigma X^2)$, where

$$\sigma = \frac{1}{2} \left(-\frac{Q + iQ_*}{Q^2} \right)^{\frac{1}{2}} \quad (24)$$

and the eigenvalue (i.e. dispersion relation) by¹⁴

$$Q(Q + i Q_*)^{\frac{1}{2}} = D. \quad (25)$$

The eigenfunction is only valid if it approaches zero as $X \rightarrow \pm \infty$. Using Eq. (25) and making use of the fact that D is positive real, we find that the eigenfunction is well behaved for $X \rightarrow \pm \infty$ [$\text{Re}(\sigma) > 0$] as long as $\text{Re}(Q)^2 > \text{Im}(Q)^2$.

If $g = 0$, Eq. (25) is the standard dispersion relation for resistive interchange modes. As g increases, the real part of Q decreases while the imaginary part increases. In the limit of $g \rightarrow \infty$,

$$Q \approx D(iQ_*)^{-\frac{1}{2}}$$

so that the condition for validity of the eigenfunction becomes marginally satisfied for $g \rightarrow \infty$; note also that $Q \rightarrow 0$ in this limit. Thus if $\Gamma_c = 0$, the theory predicts that the Hall effect reduces the growth rate of a resistive interchange mode, but does not stabilize the system for finite g . These results are summarized in Fig. 1.

It is just as easily shown that the higher order eigenfunctions have eigenfunction $\xi = H_\ell(z) e^{-z^2/2}$ for even ℓ , where $z = [(Q + iQ_*)^{1/4}/Q^{1/2}] X$, and H_ℓ are Hermite polynomials. The eigenvalues for these modes satisfy $Q(Q + iQ_*)^{1/2} = D/(2\ell + 1)$.

The remaining thing to check is the validity of the constant Ψ approximation. As we will see, it is valid if $D \ll 1$, which holds for a low β plasma. According to Eq. (24), the length scale of the eigenmode

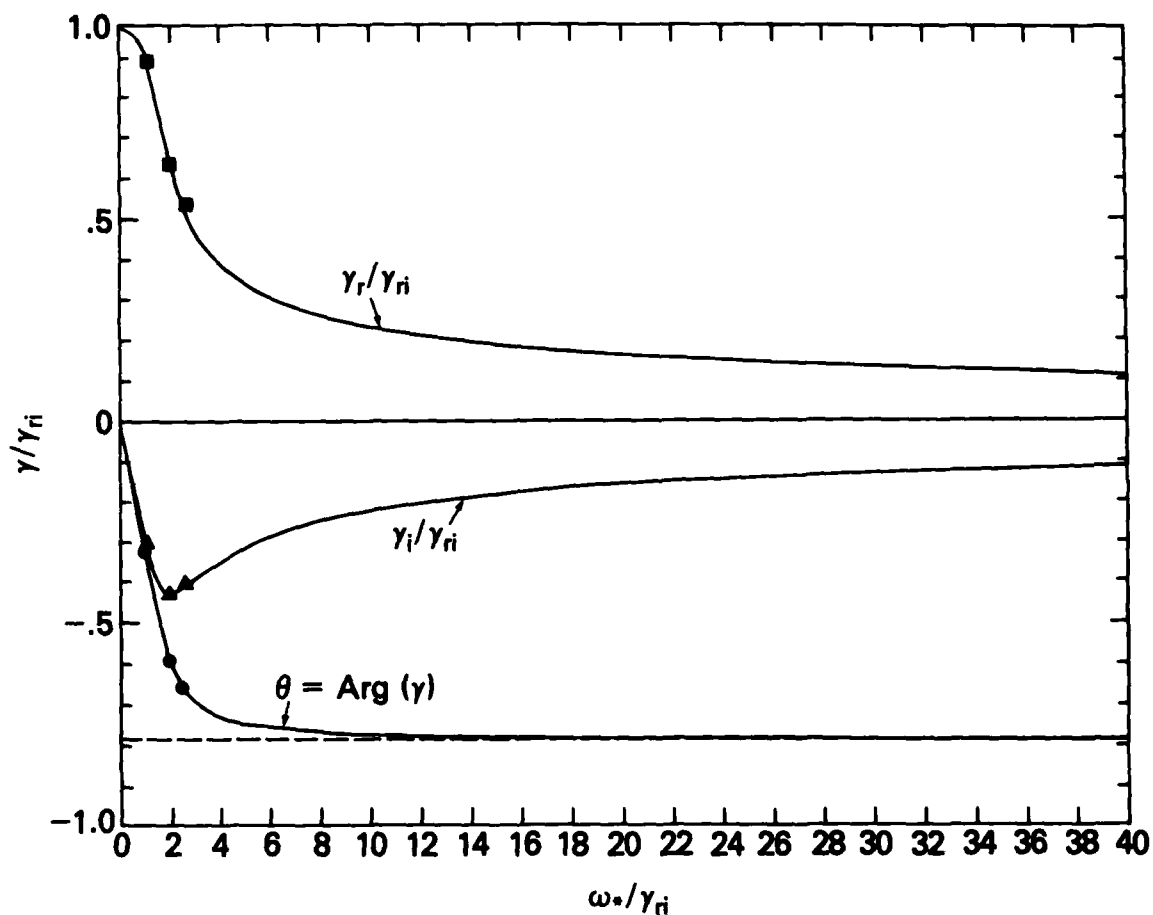


Fig. 1 - Complex growth rate Q for the drift-resistive interchange mode with $\Gamma_c \beta = 0$, given by Eq. (25). The growth rate is scaled to the pure resistive interchange value for $Q_* = 0$, i.e. $Q = D^{2/3}$, and $\epsilon = \omega_{*e}/\gamma_{ri} = Q_*/D^{2/3}$.

is $[(Q + iQ_*) / Q^2]^{-1/4}$. Using this, we find that the Ψ terms on the left and right hand side of Eq. (22) are related as $1 : (Q + iQ_*)^{1/2} Q$. Thus the left hand side of (23) dominates for $D \ll 1$, giving (to lowest order) $d^2\Psi/dX^2 = 0$.

Thus if $\Gamma_c = 0$, it is possible to derive the dispersion relation and eigenfunction for all resistive interchange modes in a cylindrical plasma. For the case of $g = 0$, they are identical to resistive interchange modes in a slab, when an artificial gravity is used in place of curvature. As g increases, the frequency behaves as in Fig. 1 (for all even l modes.) Stability is not achieved for any finite g , but the growth rate behaves as $g^{-1/2}$ as $g \rightarrow \infty$, with $|\text{Im}/Q|/|\text{Re}Q|$ approaching unity as $g \rightarrow \infty$. The latter observation implies that $\text{Re}(\sigma)$ approaches zero as $g \rightarrow \infty$ so that the outgoing drift waves are not spatially damped for $g \rightarrow \infty$.

We now consider modes with odd ξ and even Ψ which couple to the outer MHD region. The problem now is to solve Eq. (23) in which Ψ is regarded as a constant. Since we are looking for modes which do not satisfy the homogeneous equation for ξ (these are the resistive interchange modes we have just discussed), we are interested in the particular solution. This can be found most easily by Fourier transforming the equation. Multiplying by e^{ikX} and integrating over X , we find

$$-\frac{Q + iQ_*}{Q^2} \frac{d^2 \hat{\xi}}{dk^2} + k^2 \hat{\xi} - \frac{D}{Q^2} \hat{\xi} = 2\pi i \frac{Q + iQ_*}{Q^2} \Psi_0 \delta'(k) \quad (26)$$

where we have used the notation $\hat{\xi}(k) = \int_{-\infty}^{\infty} dX \xi(X) e^{ikX}$. Thus we want to solve Eq. (26) subject to the boundary condition that $\hat{\xi}$ is well behaved as $k \rightarrow \pm \infty$. Since the inhomogeneity is the derivative of a delta function, we simply solve

the homogeneous equation for $|X| > 0$ and calculate the discontinuity across $X = 0$. For $k > 0$, Eq. (26) is the equation for parabolic cylinder function. For positive k we find

$$\hat{\xi}(k) = A U(a, \kappa) \quad k > 0 \quad (27)$$

where

$$\kappa = \sqrt{2} \left(\frac{Q^2}{Q + iQ_*} \right)^{\frac{1}{4}} k, \quad (28)$$

$$a = \frac{-1}{2} \frac{D}{Q^2} \left(\frac{Q^2}{Q + iQ_*} \right)^{\frac{1}{2}}. \quad (29)$$

and A is a coefficient to be determined shortly. The function $U(a, \kappa)$ is the parabolic cylinder function (in the notation of Ref. 17) which approaches zero as κ approaches infinity along the real axis. For a conventional tearing mode, $Q_* = 0$ and Q is real, so $\hat{\xi}$ does have the proper behavior. If the Q_* terms are included, the situation, as we will see, is somewhat more complex. We must check, *a-posteriori*, that the eigenfunction derived by the dispersion relation, $U(a, \kappa)$ has the proper behavior as $\kappa \rightarrow \infty$.

Equation (27) is the functional form of $\hat{\xi}(k)$ for positive k . Since the source term on the right hand side of Eq. (26) has odd symmetry in k , $\hat{\xi}(k)$ must also be an odd function for the particular solution. Thus we find

$$\hat{\xi}(k) = -A U(a, -\kappa) \quad k < 0 \quad (30)$$

The value of A can be determined by integrating Eq. (26) across the derivative of the delta function at $k = 0$. The result is

$$A = \frac{-\pi i \Psi_0}{U(a,0)} \quad (31)$$

To summarize, the solution to the inhomogeneous equation for $\hat{\xi}(k)$, Eq. (26), is given by Eqs. (27) - (31).

To get the dispersion relation, we assume, as usual, that the outer ideal magnetohydrodynamic region specifies a value of Δ' , the discontinuity in $(d\hat{B}_r/dr)/\hat{B}_r$, across the singular layer. Matching with its counterpart from the inner region, we obtain, from Eq. (23)

$$L_r \Delta' = \int_{-\infty}^{\infty} dX (Q + iQ_*) (\Psi + X\xi) \quad (32)$$

To do the integrals over X note that $\xi(X) = \frac{1}{2\pi} \int_{-\infty}^{\infty} \hat{\xi}(k) e^{-ikX} dk$ while Ψ (assumed constant) is $\Psi_0 \int_{-\infty}^{\infty} \delta(k) e^{-ikX} dk$. Note that in doing the ξ integral over X , one will ultimately have a derivative of a delta function in the k integral.

Inserting these forms into Eq. (32) we see that both the Ψ and ξ contributions have a delta function component at $k = 0$, but these two divergent contributions cancel. This cancellation is of course the analog of the separate integrals in X space of Ψ and $X\xi$ diverging for $X \rightarrow \infty$, while the integral of $\Psi + X\xi$ converges.

The remaining part of the k integral comes from the derivative of the parabolic cylinder function at $k = 0$. The final result is

$$L_r \Delta' = 2\pi \frac{\Gamma(\frac{3}{4} + \frac{a}{2})}{\Gamma(\frac{1}{4} + \frac{a}{2})} (Q + iQ_*)^{\frac{3}{4}} Q^{\frac{1}{2}} \quad (33)$$

If D and Q_* are both equal to zero, this is the standard dispersion relation for the tearing mode. To get the growth rate with $Q_* \neq 0$, the procedure is to solve Eq. (33) and remain on the branch which gives the tearing mode as $Q_* \rightarrow 0$. For $D = a = 0$, this gives the standard drift tearing dispersion relation^{14,15}

$(Q + iQ_*)^{3/4} Q^{1/2} = Q_t^{5/4}$, where Q_t is the pure ($Q_* = 0$) tearing mode growth rate. However we must also check that this branch is well behaved as X or $k \rightarrow \infty$. This requires that the real part of σ [c.f. Eq. (24)] remains positive. Inserting for $Q + iQ_*$ from the dispersion relation, with $D = 0$, we find that this means

$$\phi > -\frac{3\pi}{8} \quad (34)$$

where $\tan(\phi) = \text{Re}(Q)/\text{Im}(Q)$. As shown in Fig. 2, the dispersion relation does approach this point while the mode is unstable¹⁵, so that at this point, the instability abruptly disappears, or possibly shifts to another branch of the dispersion relation. However, we also show in the next section that if the d^2T/dX^2 terms are included, the growth rate can be brought to zero by increasing Q_* while the eigenfunction remains well behaved.

For $D > 0$, the dispersion relation to Eq. (33) gives other solutions of a more interchange - like nature. For example, for $\Delta' \rightarrow \infty$ we obtain roots associated with poles of the Γ function in the numerator, $Q(Q + iQ_*)^{1/2} = D/(2\ell + 1)$, where ℓ is now odd. For $\Delta' \rightarrow 0$ we obtain $Q(Q + iQ_*)^{1/2} = D/(2\ell - 1)$, again only for odd ℓ .

We now continue with our examination of analytic solutions of Eqs. (16) - (18). We first make the constant Ψ approximation, and begin by looking at homogeneous solutions to Eqs. (16) and (18) [i.e. with $\Psi = 0$] in the limit of large X . Keeping only second derivatives and terms proportional to X^2 we find that the equations reduce to

$$\frac{d^2\xi}{dX^2} = \frac{X^2}{Q} \xi + \frac{2ig}{SQ^2} X^2 T \quad (35)$$

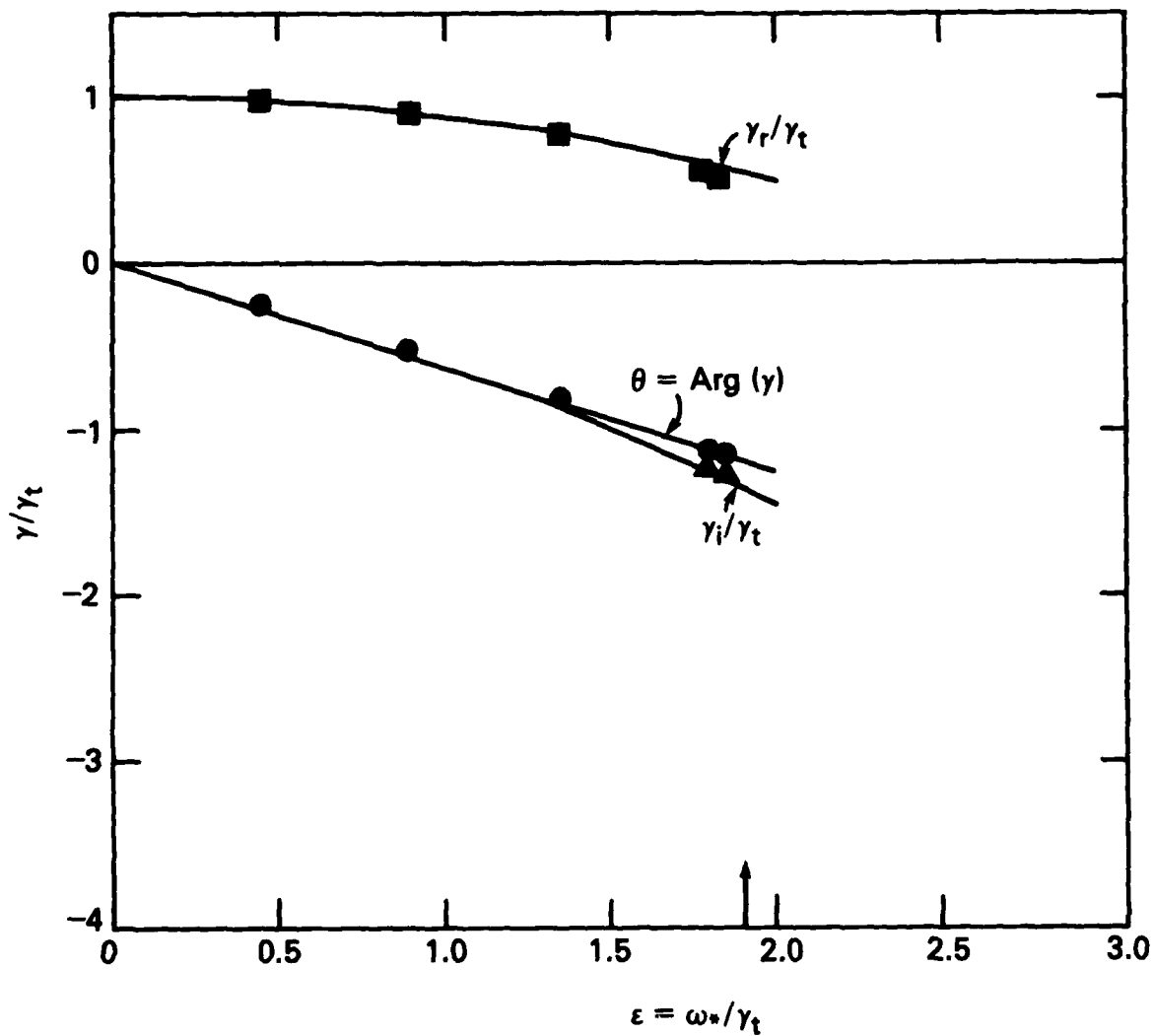


Fig. 2 - Complex growth rate for the drift-tearing mode with $\Gamma_c \beta = 0$, from (33) with $D = 0$. Again, Q and Q_* are normalized by the pure tearing mode growth rate $Q = (L_r \Delta / 2.12)^{4/5}$.

$$\frac{d^2 T}{dx^2} = \frac{X^2}{Q} T - 2iQ^2 g \xi. \quad (36)$$

In the limit of large X , we assume that spatial variations are as $\exp(-\sigma X^2)$. Using this spatial dependence and taking $X \rightarrow \infty$, Eqs. (35) and (36) reduce to

$$4\sigma^2 \xi_0 = \frac{\xi_0}{Q} + \frac{2ig}{SQ^2} T_0 \quad (37)$$

$$4\sigma^2 T_0 = \frac{T_0}{Q} - 8i Q^2 g \sigma^2 \xi_0 \quad (38)$$

so that we obtain four solutions

$$\sigma = \pm \left[\frac{g}{2\sqrt{S}} \pm \frac{1}{2} \left(\frac{g^2}{S} + \frac{1}{Q} \right)^{\frac{1}{2}} \right] \quad (39)$$

The two expressions for σ are quite different in magnitude as long as $\frac{g^2}{S} \gg \frac{1}{Q}$. In the limit of large g , we expect the frequency to be roughly a drift wave frequency $|Q| \sim Q_* \sim \beta g$, so that the roots are well separated if $S \sim 1$ and

$$g^3 \beta \gg 1 \quad (40)$$

We will assume Eq. (40) is satisfied, and also that $Q \sim \beta g$ and $S \sim 1$ and examine analytic solutions of Eqs. (16) - (18) which do not couple to the outer MHD region, i.e. for even ξ , T and odd Ψ . Taking the negative sign inside the bracket in Eq. (39), we find

$$\sigma = \frac{S^{\frac{1}{2}}}{4gQ} \quad (41)$$

Notice that if Q is purely imaginary, as it nearly is for a drift wave, to lowest

order the exponential does not decay in space, but oscillates more and more rapidly. However on keeping next order terms in the expansion of $(\frac{g^2}{S} + \frac{1}{Q})^{1/2}$, one can easily show that σ has a real part even if Q is purely imaginary. Thus it is possible to have spatially localized shear damped drift waves (i.e. real part of $\sigma > 0$ and $R_e(Q) < 0$.) In the next section we show that this is indeed the case.

To continue, we will assume lengths are scaled by the σ given in Eq. (41) with $Q \sim g\beta$ so that $X \sim (gQ)^{1/2} \sim g\beta^{1/2}$ and $\frac{d}{dX} \sim g^{-1}\beta^{-1/2}$. Then, comparing the terms in Eqs. (16) and (17) and using $1/g^3\beta$ as a small parameter, we find that (16) and (17) reduce to

$$QX \xi + \frac{2ig}{S} X T = 0, \quad (42)$$

a simple algebraic relation between ξ and T . Using this, and using the same ordering on Eq. (18) we find that it reduces to a Weber equation

$$\frac{4Qg^2}{S} \frac{d^2T}{dX^2} = \frac{X^2}{Q} T + \left[\frac{2Q}{\Gamma\beta} + \left(S - \frac{2D}{\Gamma\beta} \right) \left(\frac{-2ig}{S} \right) \right] T = 0 \quad (43)$$

where we have assumed $T_1 = 0$, and also assumed $\frac{2}{\Gamma\beta} \gg 1$. If S were equal to zero, the term in the square brackets would be proportional to the drift wave dispersion relation $Q + iQ_* = 0$ where $Q_* = \frac{2gD}{S}$. The effect of the S term is to lower the drift wave frequency for $D > 0$ (that is for "bad" curvature). With the d^2T/dX^2 and X^2T terms included, Eq. (43) gives the dispersion relation for shear stabilized drift waves. Assuming $Q = -i\omega_D \equiv -iQ_* + i\Gamma\beta g$ in the d^2T/dX^2 and X^2T terms and outgoing wave boundary conditions, we find the dispersion relation is

$$\frac{2Q}{\Gamma\beta} + (S - \frac{2D}{\Gamma_c\beta}) (\frac{-21g}{S}) = -2g(2l+1)/S^{\frac{1}{2}} \quad (44)$$

for l even. If the shear length is taken as $L_s^{-1} = |aq'/Rq^2|$ and $|\frac{p}{p'}| = |\frac{\rho}{\rho'}| = L_n^{-1}$, $\Gamma_c = 1$ for isothermal electrons,

$$\frac{\text{Re}(Q)}{Q_*} = \frac{\text{Re}(\gamma)}{|\omega_{*e}|} = \frac{-L_n B_z^2}{L_s B^2} (2l+1) \quad (45)$$

For a slab plasma in which $B_z \approx B$, the damping rate is the classical result for shear damping of a fluid drift wave in slab geometry.¹⁸ Thus in the limit of $g^3\beta \gg 1$, one of the even ξ , T , odd Ψ modes is the shear stabilized (damped) drift wave.

The condition for the validity of the constant Ψ approximation for this ordering, i.e. the condition for the dominance of the left hand side of Eq. (17), is easily seen to be $g^3\beta^2 \ll 1$.

We will continue by considering the other choice for spatial scale length in Eq. (39),

$$\alpha = \frac{B}{\sqrt{S}} \quad (46)$$

which corresponds to a much more spatially localized mode than the shear stabilized drift wave. Assuming $d/dX \sim g^{1/2}/s^{1/4}$, $X \sim S^{1/4}/g^{1/2}$,

$Q \sim \beta g$ and $g^3\beta \gg 1$, we once again examine Eqs. (16) and (18) (assuming again $\Psi = 0$; in this ordering the constant Ψ approximation requires $\beta \ll 1$) and pick out the dominant terms. They are

$$\frac{d^2\xi}{dX^2} = \frac{21gX^2}{SQ^2} T - \frac{1}{Q^2} T \quad (47)$$

$$\frac{d^2 T}{dX^2} = \frac{2Q}{\Gamma_c \beta} T - 2iQ^2 \frac{d^2 \xi}{dX^2} \quad (48)$$

Combining these to form a single equation for T , we again arrive at a Weber equation

$$\frac{d^2 T}{d\xi^2} = \frac{4g^2 X^2}{S} T + \left(\frac{2Q}{\Gamma_c \beta} + 2ig \right) T = 0, \quad (49)$$

the eigenvalues of which are

$$Q = -i\Gamma\beta g - \Gamma_c \beta |g| (2\ell + 1)/S^{\frac{1}{2}} \quad (50)$$

for even ℓ . Again the result is a damped mode with a real frequency of order the drift frequency.

Thus as the plasma becomes more and more collisionless (that is as $g \rightarrow \infty$) all localized (i.e. even ξ , T , odd Ψ) unstable modes disappear. Hence a localized resistive interchange mode which is unstable for $g = 0$ must be damped as $g \rightarrow \infty$ if it remains a localized mode. This is an interesting and useful result which is not so for the simplest case of $\Gamma_c = 0$. In that case, as we showed earlier in this section, the unstable resistive interchange mode persists as $g \rightarrow \infty$. Thus it is not only the Hall effect, but also plasma compressibility which needed to stabilize localized resistive interchange modes in a cylindrical plasma.

In the next section we show by a numerical study of Eqs. (16) - (18) that localized resistive interchange modes are indeed stabilized as $g \rightarrow \infty$. However this conclusion seems to be even more general. We find that both tearing modes with positive Δ' and resistive interchange modes which couple to the outer ideal magnetohydrodynamic region (but have $\Delta' < 0$) are all stabilized by increasing g .

Furthermore, as shown in the Appendix, odd ξ , T , even Ψ modes can be stabilized for positive Δ if g is large enough.

IV. Numerical Results

In this section we describe results obtained by integrating Eqs. (16) - (18) numerically. We integrate the full sixth order set, because the conditions for the validity of the constant - Ψ approximation cannot be assured to hold for all values of g . Indeed, in the drift wave region this criterion, $g^3 \beta^2 \ll 1$, holds only marginally for values of interest. Nevertheless, we integrate only the singular layer equations, using a higher order version of the Δ' method usually used in conjunction with the constant - Ψ approximation. Specifically, we obtain from (16) - (18) the first two terms in the asymptotic series relating ξ and T to Ψ at large X :

$$\xi \rightarrow - [1 + (D/Q + 2igQ)/X^2] \Psi/X, \quad (51)$$

$$T \rightarrow - [1 - SQ^2/DX^2] D\Psi/X. \quad (52)$$

Using these expressions in the annihilated equation of motion, we compute the symmetric and antisymmetric components of Ψ , which for large positive X are given by

$$\begin{aligned} \Psi_s &\rightarrow \Psi_0 [1 + D \ln X + D^2 \ln X \\ &+ D^2 (\ln X)^2 / 2] + (S-2) \Psi_0 Q^2 / 6X^2, \\ \Psi_a &\rightarrow \Psi_0' X [1 - D \ln X - D^2 \ln X \\ &+ D^2 (\ln X)^2 / 2] + S \Psi_0' Q^2 / 2X. \end{aligned} \quad (53)$$

The first terms in Ψ_s and Ψ_a are, respectively, the expansion for small D of the

exterior Suydam solutions (for $D < \frac{1}{4}$) $\psi_0 X^{q_1}$ and $\psi_0' X^{q_2}$ where $q_{1,2} = [1 \mp (1-4D)^{1/2}]/2$. We match ψ'/ψ to the outer (ideal magnetohydrodynamic) region by means of two parameters $\delta_{r,\ell} = b\psi_0'/a\psi_0$ (δ_r for $X \rightarrow +\infty$ and δ_ℓ for $X \rightarrow -\infty$), where ψ is assumed to be given by $\psi = a\psi_s + b\psi_a$. The advantage of taking the higher order terms in the asymptotic expansion in (53) is that we can then perform the numerical integrations over a relatively small interval in X .

We first discuss numerical solutions which correspond to the analytic solutions of Refs. 3, 7 ($g = 0$) and Sec. III ($\Gamma_c = 0$).

Figure 3 shows the results obtained by this code for the odd ξ tearing resistive interchange with $g = 0$ and $\Delta' < 0$. For very small D , we see that the $Q = (2.12\pi D/4L_r \Delta')^4$ scaling of Ref. 7 holds, showing a much smaller growth rate than the conventional ($\Delta' = 0$) value $Q = (\pi D/4)^{2/3}$. For larger D the assumption $2D/\Gamma\beta \ll 1$, in which compressional stabilization is a dominant effect, breaks down and the growth rates found by the code are larger than those found in Ref. 7. Nevertheless, for reasonable values of the Suydam parameter D , the growth rate is still considerably smaller than the conventional value $(\pi D/4)^{2/3}$. By increasing D while keeping all other parameters fixed, we pass through five distinct regions, the $(D/\Delta')^4$ regime of Ref. 7, a transition regime due to the diminished stabilizing effect of plasma compression, the classical $D^{2/3}$ regime, a regime where the constant ψ approximation breaks down and finally $D \rightarrow 1/4$, where the mode becomes unstable in ideal magnetohydrodynamics. For realistic parameters (e.g. for a reversed field pinch) these regimes overlap so strongly that the individual regimes cannot be unequivocally recognized in the numerical results.

We have also used the code with $L_r \delta_r = .02$, $L_r \delta_\ell = -.02$ ($L_r \Delta' = +.04$), $\Gamma\beta = 10^{-5}$, $D = 10^{-3}$ and $S = 0.1$ to investigate the low beta drift tearing mode discussed in Sec. III. We find excellent agreement in growth rate and in real

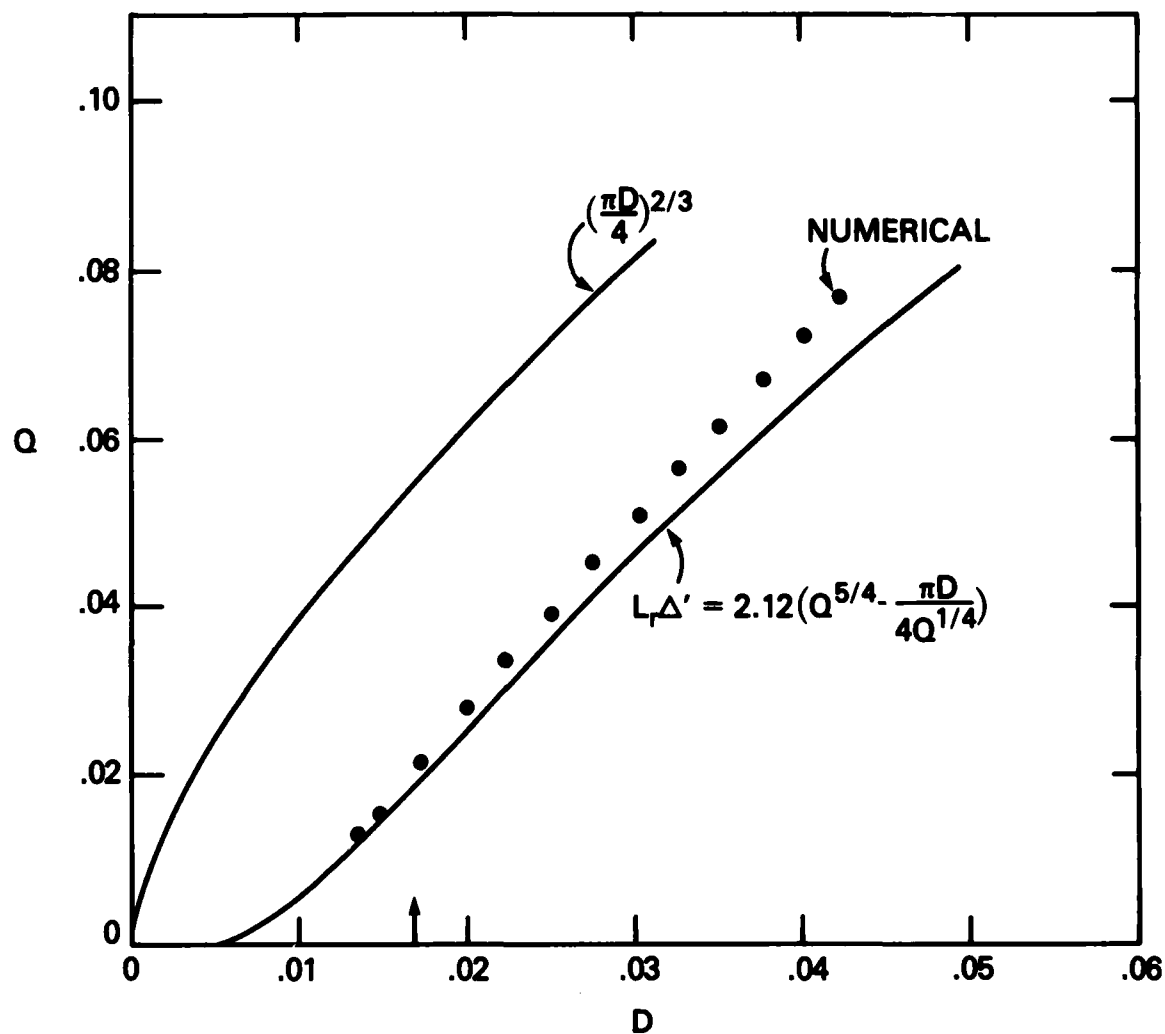


Fig. 3 - Growth rate of even Ψ , odd ξ , T resistive interchange mode as a function of the Suydam parameter D , with $L_r \Delta' = -0.06$, $S = 0.1$, $\Gamma_c \beta = 0.1$.

part of frequency up to the point $\varepsilon \equiv \omega_*/\gamma_t = 1.89$ (γ_t is the $g = 0$ tearing mode growth rate) or $g = 4.21$, where there is no spatial damping as $X \rightarrow \infty$, i.e. σ [of eq. (24)] is pure imaginary. These results are shown in Fig. 2.

We have also studied a low $\Gamma\beta$, $\Delta' = 0$, even ξ resistive interchange and found that the numerical results were in excellent agreement with (25), which shows that the unstable resistive interchange approaches marginal stability as $g \rightarrow \infty$ ($\omega_* \rightarrow \infty$), and that $\text{Re}(\sigma)$ [of Eq. (24)] approaches zero, i.e., $\theta \equiv \text{Arg } \gamma$ approaches $-\pi/4$, as $g \rightarrow \infty$. These results are summarized in Fig. 1.

We now turn to a study of drift resistive interchange and drift tearing modes in a cylindrical plasma with parameters relevant to current reversed field pinch experiments. Nominal values of density, temperature, and magnetic field of $n = 2 \times 10^{14} \text{ cm}^{-3}$, $T_e \sim T_i = 100 \text{ eV}$, and $B = 4 \text{ kg}$ are used. We fix $\Gamma\beta = 0.167$ in the code, consistent with the above parameters. We have observed, as first noted by Greene,¹⁹ that for fairly high beta (more than a few percent) and fixed D , the stability results are relatively insensitive to β (and therefore insensitive to the difference between an isothermal and an adiabatic equation of state). Assuming Bessel function profiles $B_\theta = J_1(\mu r)$, $B_z = J_0(\mu r)$, with $2.4 < \mu r_w < 3.1$ (r_w is the radius of the conducting wall), we find $q R = -\mu a = -2.4$, is again the radius of the mode rational surface. We have assumed that a is at the field null, as is appropriate for $m = 0$ modes. We obtain $S = 0.7$. For stability to all localized resistive interchanges with $g = 0$, we pick $S - 2D/\Gamma\beta = -1$, or $D = 0.14$. As discussed in Ref. 7, this condition gives reasonable pressure profiles with a finite but very small pressure at the wall. A typical value for R_m , the magnetic Reynolds' number, for radial scale lengths $5 - 10 \text{ cm}$, is $R_m = 10^6$, and for $2.4 < \mu r_w < 3.1$, $\Delta' r_w \sim -5$ for $m = 0$.

and $m = 1$ modes (the latter with their mode rational surface inside the field null). We find $L_r \Delta' \sim -.06$, and $g = 5$.

In Fig. 4 we show the complex growth rate Q as a function of g , for the odd ξ , T , even Ψ mode, with all the other parameters given in the previous paragraph. We also show the line $\omega = \omega_*$ or $Q = -iQ_*$. We see that $\omega/\omega_* \approx 1/2$ throughout the unstable range and that this mode is stabilized for $g > 2.35$, well below the nominal value of this parameter for reversed field pinches. The mode structure for various values of g is shown in Figs. 5-8. For $g = 0.5$, as seen in Fig. 5, ξ , T , and Ψ have real parts resembling $g = 0$ resistive interchanges, but also have imaginary parts. For $g = 2.0, 2.25, 2.40$ (Figs. 6-8), one can see evidence of the localized behavior in T due to perpendicular resistivity and also evidence of outgoing propagating drift waves. (It is easily seen in Figs. 6-8 that the radial phase velocity is inward, and we know from the local dispersion for drift waves in a sheared geometry¹⁸ that the radial group velocity is in the opposite direction, corresponding to an outgoing wave boundary condition.)

We have also studied the even ξ resistive interchange with smallest radial mode number $l = 0$ (i.e. no nodes for $\omega_* = 0$). We pick all parameters the same as for the odd ξ mode, except $\Gamma\beta = 0.0512$, so that with $g = 0$ the two modes have the same growth rate. (By decreasing $\Gamma\beta$ without changing D we decrease the stabilizing influence of plasma compression.) This mode is then stabilized for $g = 4.0$, as shown in Fig. 9. This larger value is required presumably because this more localized mode is more weakly coupled to outgoing drift waves. For small g we observe $\omega_r \approx \omega_*/3$. The mode structure at marginal stability is shown in Fig. 10. Again evidence for localized behavior due to perpendicular resistivity and drift wave behavior at larger X is present, and the apparent radial phase velocity is negative, indicating an outward propagation of energy.

We have also investigated cases in which $\kappa \neq 0$, i.e. when the ion temperature gradient is smaller ($\kappa < 0$) or larger ($\kappa > 0$) than that of the baroclinic profile $T_i \sim \rho^{\Gamma-1}$. We find that increasing ion temperature gradient is a stabilizing influence. However, these results do not necessarily have immediate implications for devices with $T_i \sim T_e$ because we have neglected the collisionless ion viscosity and thermal conduction terms, which are of the same order of magnitude.

We have also investigated the odd ξ mode of Figs. 4-8 for $\Delta' > 0$, where it goes over to a tearing mode. As seen in Fig. 11 the value of g required for stability increases very slowly with Δ' . These results are in qualitative agreement with the results shown in the Appendix, which show that this mode can be stable for positive Δ' .

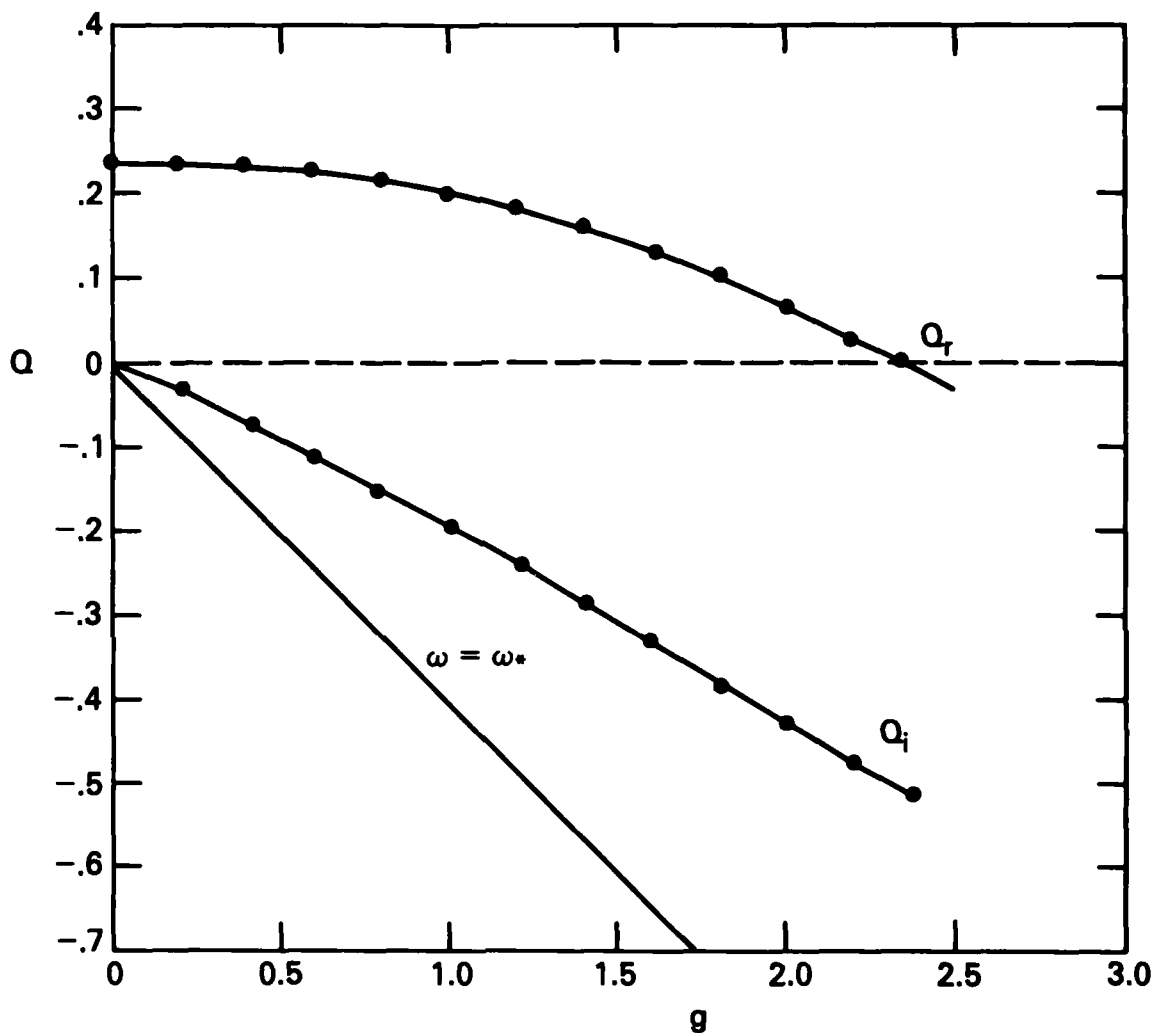


Fig. 4 - Complex growth rate for odd ξ resistive interchange (tearing) mode as a function of g , with $L_r \Delta' = -0.06$, $S = 0.7$, $\Gamma_c \beta = 0.167$, $D = 0.14$.

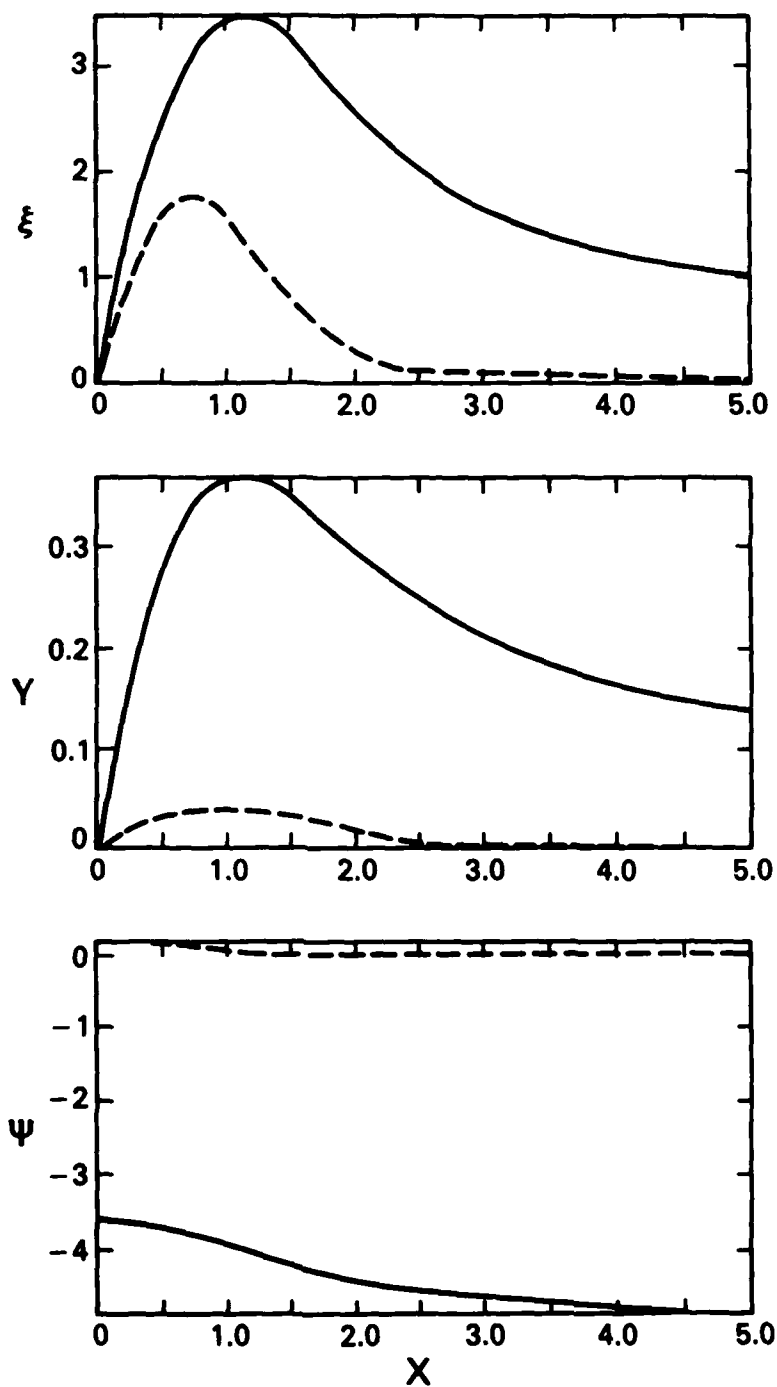


Fig. 5 - Eigenfunctions (ξ , T , ψ) for the case of Fig. 4, with $g = 0.5$.

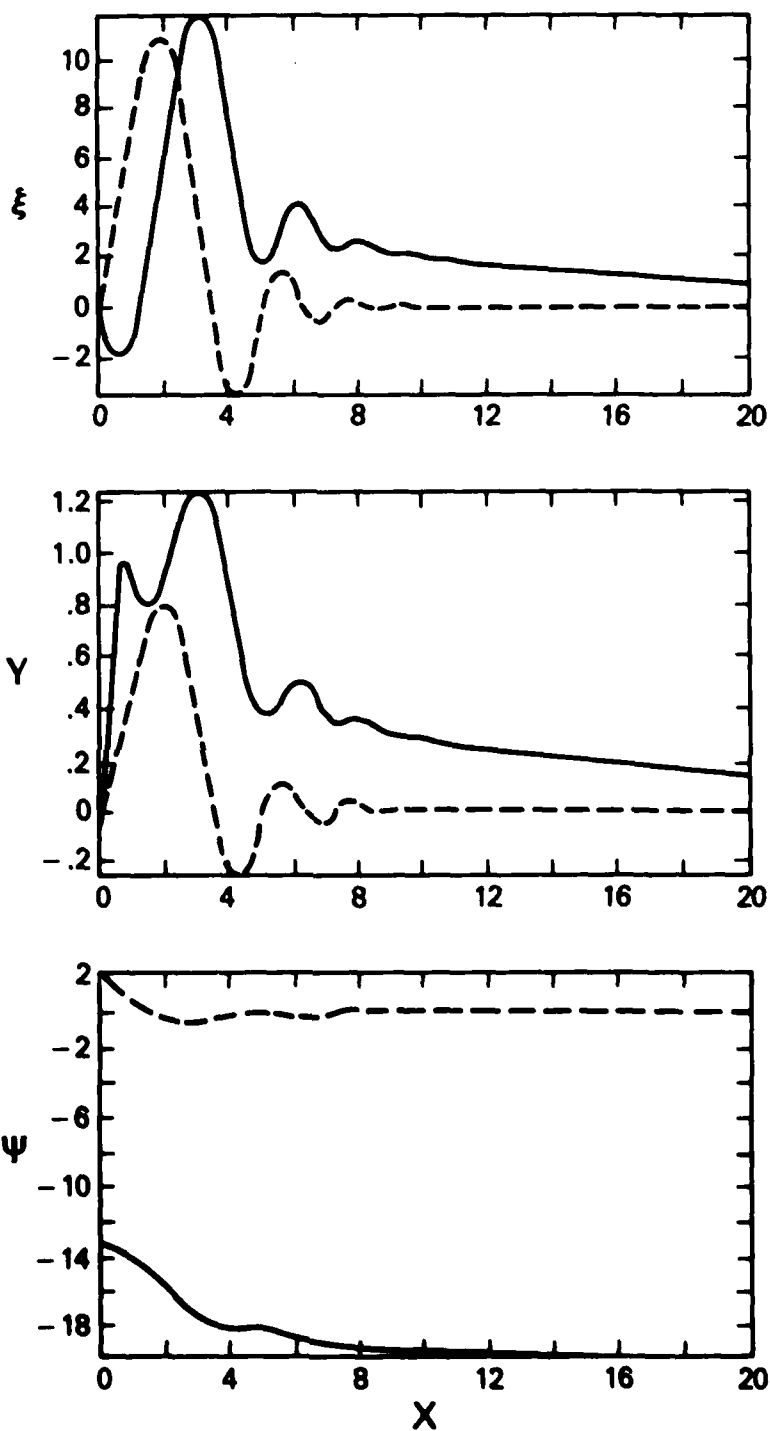


Fig. 6 - Eigenfunctions for $g = 2.0$.

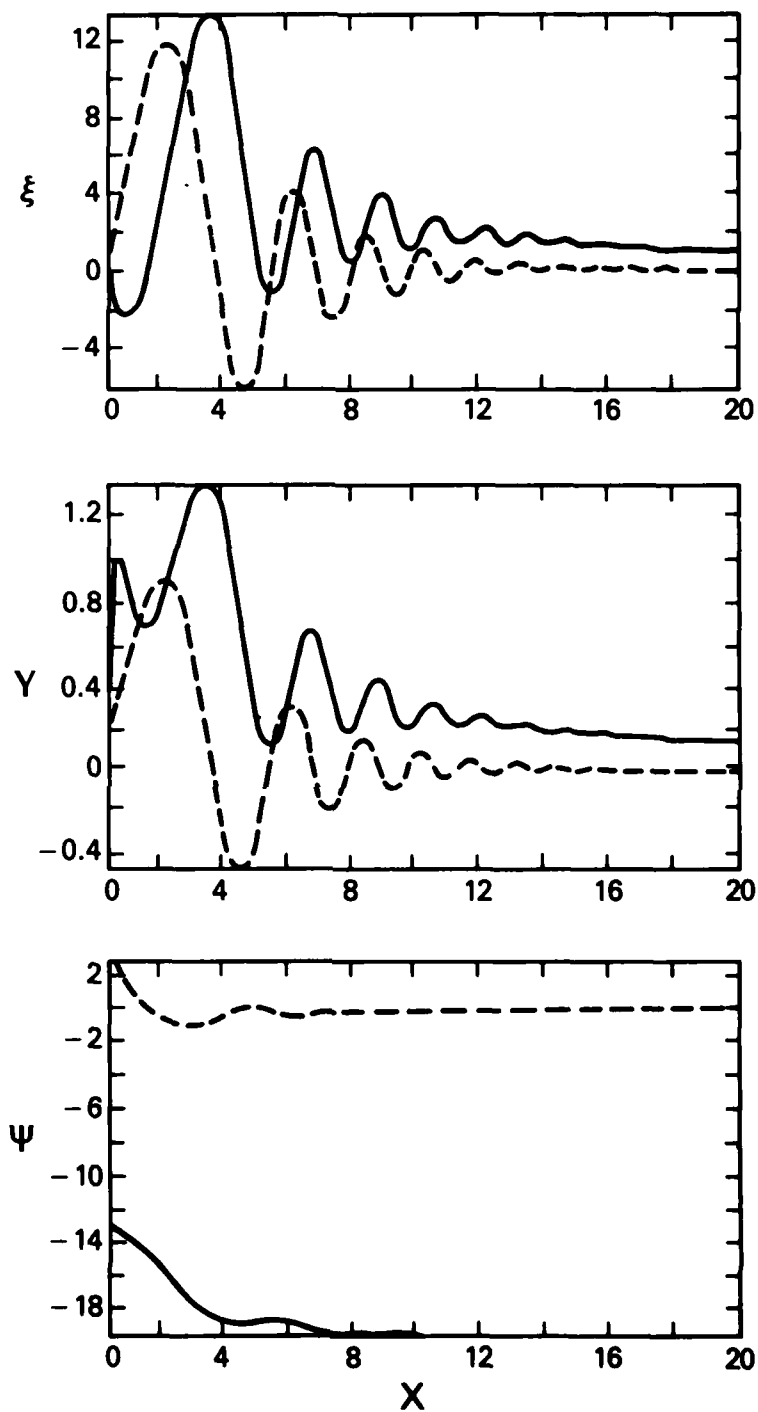


Fig. 7 - Eigenfunctions for $g = 2.25$.

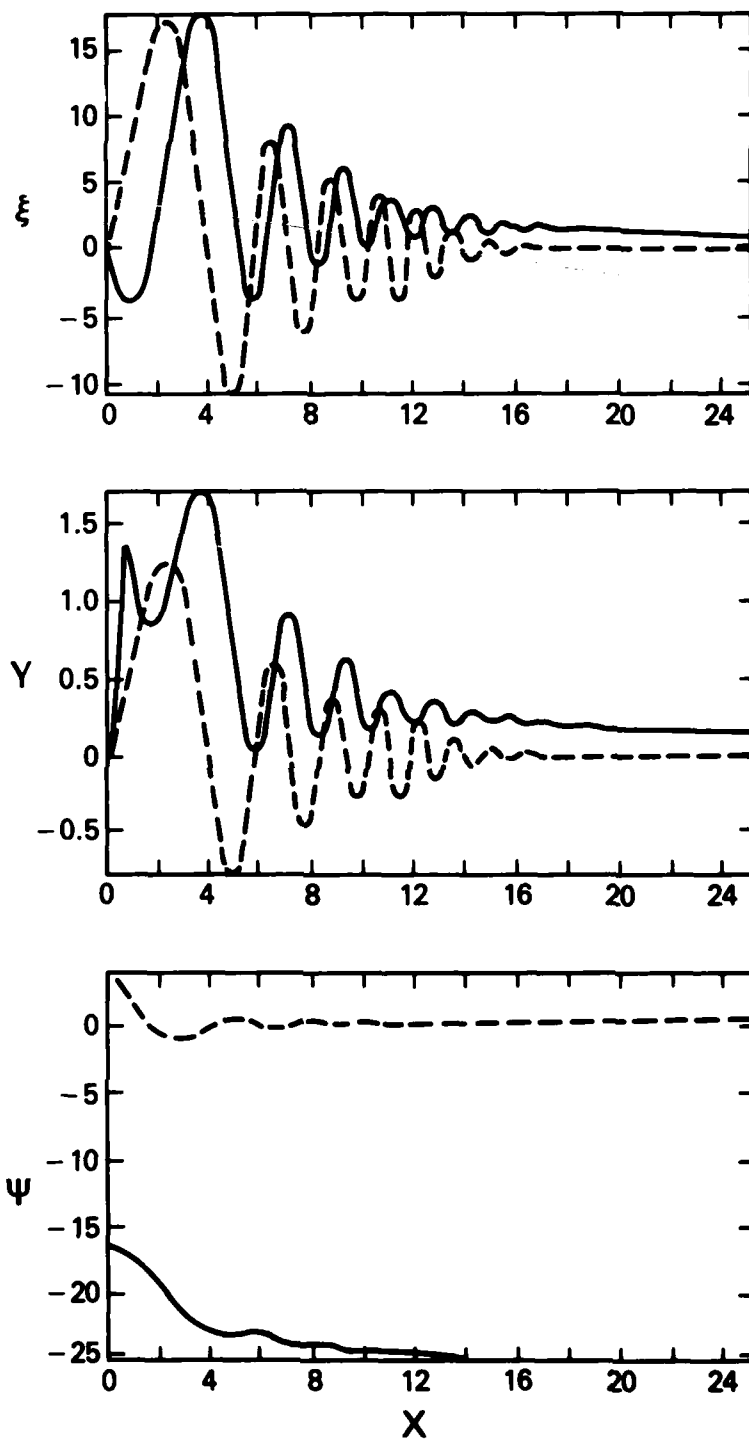


Fig. 8 - Eigenfunctions for $g = 2.40$.

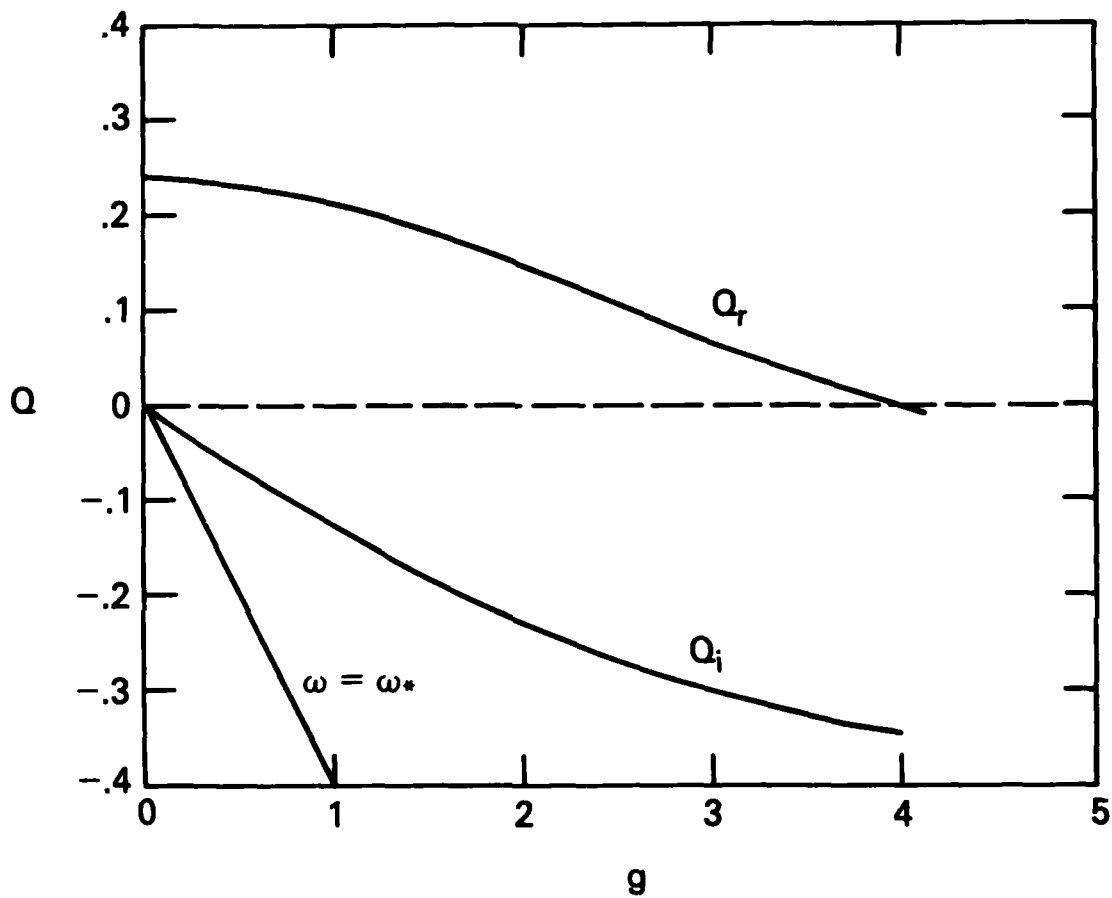


Fig. 9 - Complex growth rate for even ξ resistive interchange mode ($l = 0$) as a function of g with $L_r \Delta' = 0$, $S = 0.7$, $\Gamma_c \beta = 0.0512$, $D = 0.14$.

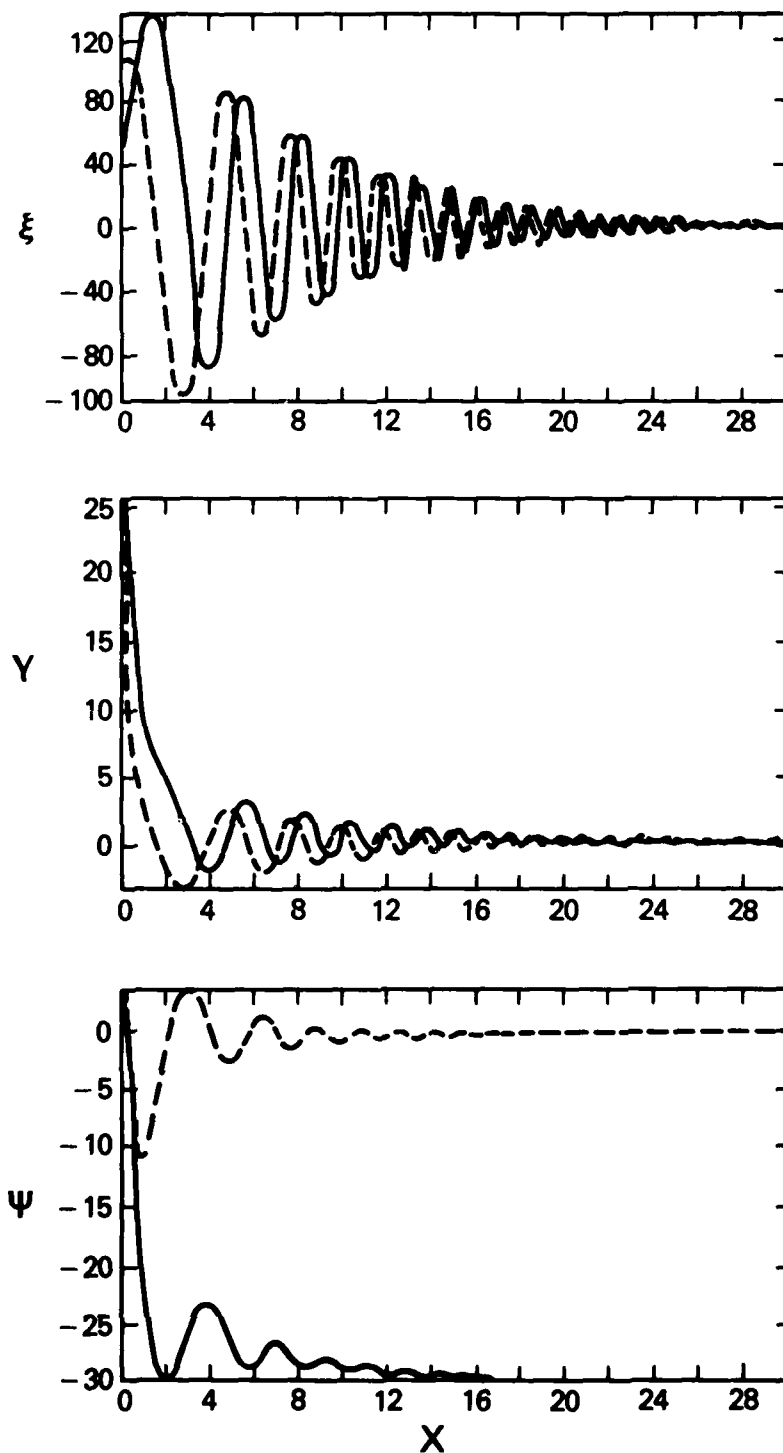


Fig. 10 - Eigenfunctions (ξ , T , ψ) for the case of Fig. 9, with $g = 4.0$ (at marginal stability).

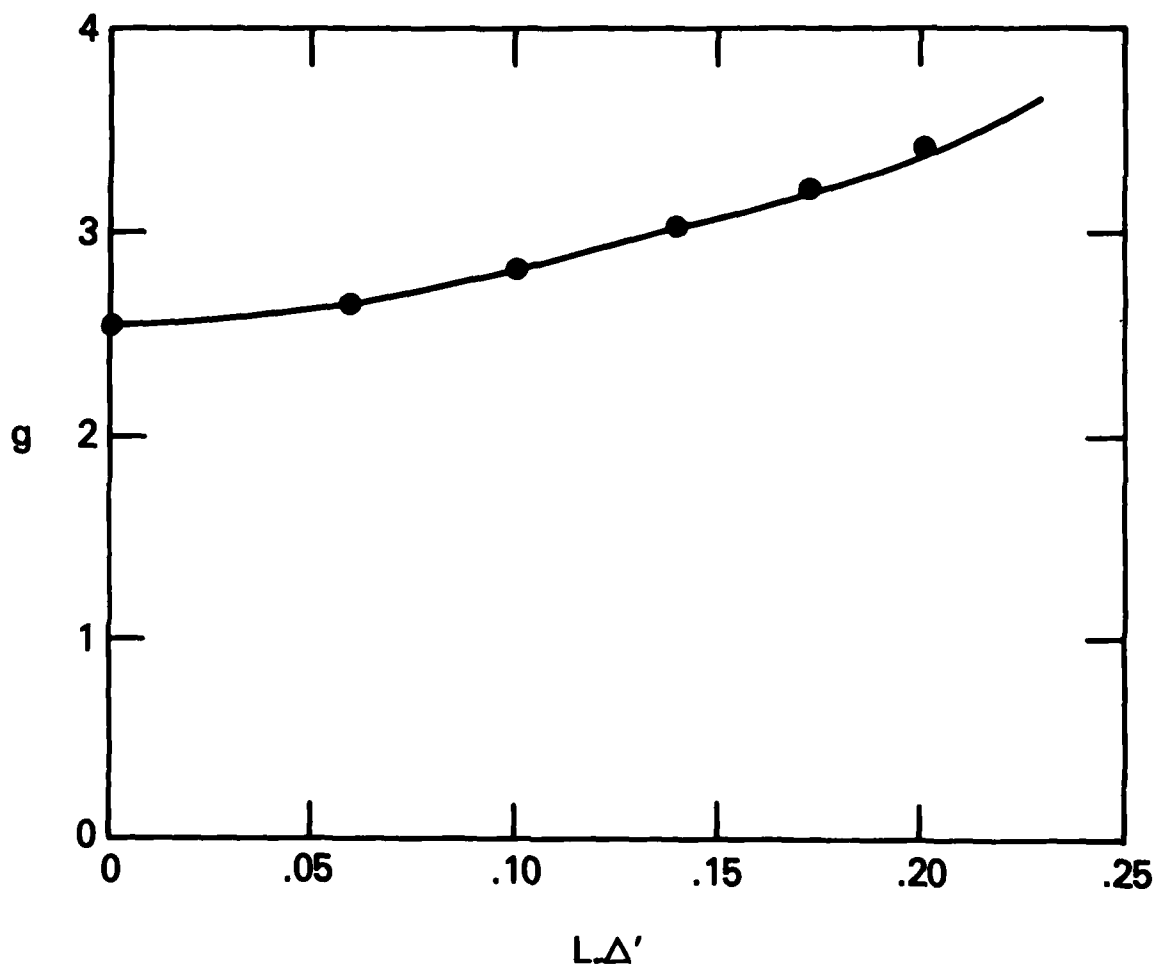


Fig. 11 - Value of g required for marginal stability of the odd ξ (tearing) mode as a function of Δ' , for $S = 0.7$, $\Gamma\beta = 0.167$, $D = 0.14$.

V. Conclusions

We have analyzed the stability of tearing and resistive interchange modes in cylindrical geometry for parameters relevant to current reversed field pinch experiments. Our principal conclusions are that these modes are strongly stabilized by the inclusion of the Hall terms in Ohm's law, the retention of plasma compression, and exact treatment of field line curvature. The same results are not obtained from a slab model which includes Hall terms but models field line curvature with a fictitious gravity.

In the derivation of the governing equations we made two approximations which if relaxed may modify our results. The first of these was the neglect of the equilibrium electron temperature gradient and electron thermal conductivity. Analysis of tearing modes in slab geometry has indicated a strong stabilizing effect associated with the equilibrium temperature gradient.^{21,22}

The second approximation was $T_i \ll T_e$, which allowed us to neglect gyroviscosity, and the gyro-heat flux. In addition we often assumed $\kappa = 0$. These approximations have the effect of eliminating from considerations localized drift modes which are driven by the ion temperature gradient²³ and drift modes which are driven unstable by unfavorable ion curvature drifts.

Nevertheless, we have seen that the modes which evolve from the interchange and tearing modes of a collisional plasma become stable as the collisionality is decreased and the Hall terms become important.

ACKNOWLEDGMENTS

We have benefitted from discussions with J. Drake, P. N. Guzdar, R. Marchand, and D. Schnack. This work was supported by Department of Energy Contract No. EX-76-A-34-1006.

REFERENCES

1. H. P. Furth, J. Killeen and M. N. Rosenbluth, Phys. Fluids 6, 459 (1963).
2. J. L. Johnson, J. M. Greene and B. Coppi, Phys. Fluids 6, 1169 (1963).
3. B. Coppi, J. M. Greene and J. L. Johnson, Nucl. Fusion 6, 101 (1966).
4. B. R. Suydam, Proc. U. N. International Conf. on Peaceful Uses of Atomic Energy, Geneva, Vol. 31, pp. 157-159, Columbia Univ. Press, New York (1959).
5. J. M. Greene and J. L. Johnson, Phys. Fluids 5, 510 (1962).
6. C. Mercier, Nucl. Fusion Suppl. Part 2, 801 (1962).
7. J. M. Finn and W. M. Manheimer, NRL Memo Rept. 4520 (to appear in Phys. Fluids.)
8. D. Schnack, J. Killeen and R. Gerwin, Lawrence Livermore National Laboratory Report #UCRL-84301 (1981), to appear in Nucl. Fusion.
9. W. M. Manheimer, Phys. Rev. Lett. 45, 1249 (1980).
10. C. J. Buchenauer, R. G. Watt, K. S. Thomas and L. C. Burkhardt, Bull. Am. Phys. Soc. 26, 1040 (1981).
11. S. C. Jardin, R. C. Grimm, M. S. Chance, R. L. Dewar, J. L. Johnson and D. A. Monticello, Bull. Am. Phys. Soc. 25, 861 (1980).
12. J. M. Finn, Bull. Am. Phys. Soc. 25, 830 (1980); J. Finn and A. Reiman, Phys. Rev. A. 24 2835 (1981).
13. S. C. Jardin, personal communication (1981).
14. R. J. Tayler, J. Nucl. Energy, Pt. C 5, 345 (1963); B. Coppi, Phys. Fluids 7, 1501 (1964).
15. P. H. Rutherford and H. P. Furth, Princeton University Report MATT-872 (1971).

16. D. W. Ross and S. M. Mahajan, Phys. Rev. Lett. 40, 328 (1978); K. T. Tsang, T. J. Catto, J. C. Whitson and J. Smith, Phys. Rev. Lett. 40, 327 (1978); T. M. Antonsen, Jr., Phys. Rev. Lett. 41, 33 (1978); L. Chen, T. N. Guzdar, R. B. White, P. K. Kaw, C. R. Oberman, Phys. Rev. Lett. 41, 649 (1978); L. Chen, T. N. Guzdar, J. Y. Hsu, P. K. Kaw, C. R. Oberman, R. B. White, Nucl. Fusion 19, 373 (1979).
17. M. Abramowitz and I. Stegun, Handbook of Mathematical Functions, NBS, Washington, D.C. (1970).
18. W. M. Manheimer, An Introduction to Trapped-Particle Instability in Tokamaks, pp. 29-32, ERDA, Washington, D.C. (1977).
19. J. M. Greene, Introduction to Resistive Instabilities, Lausanne report LRP 114/76, p. 81 (1976).
20. M. N. Bussac, D. Edery, R. Pellat and J. L. Soule, Phys. Rev. Lett. 40, 1500 (1978).
21. B. Coppi, J. W.-K. Mark, L. Sugiyama and G. Bertin, Phys. Rev. Lett. 42, 1058 (1979); ---, Ann. Phys. 119, 370 (1979).
22. J. F. Drake, N. T. Gladd, and A. B. Hassam, Bull. Am. Phys. Soc. 26, 961 (1981).
23. I. Rudakov, R. Z. Sagdeev, Dokl. Akad. Nauk SSSR 138, 581 (1961); --- Sov. Phys. Dokl. 7, 417 (1961).

APPENDIX

In this appendix we examine the approximate analytic solution of Eqs. (16) - (18) for modes that couple to the outer region for the case in which $g^3 \beta \gg 1$. The modes that we consider have even Ψ and odd ξ and T . We recall that modes with the opposite parity were treated in Sec. III, where it was found that the constant Ψ approximation is valid provided $g^3 \beta^2 \ll 1$. We will assume again that the constant Ψ approximation is valid, and thus, our results are restricted to low values of β .

In the inner region Ψ consists of a constant Ψ_0 plus a correction Ψ_1 . We integrate the second derivative of the correction given by Eq. (16) over the inner region and match to the outer solution $\Psi \sim \Psi_0 (1 + 1/2 |X| L_r \Delta^r)$ obtaining,

$$\int_{-\infty}^{\infty} dX \, d^2 \Psi_1 / dX^2 = L_r \Delta^r \Psi_0 = \int_{-\infty}^{\infty} \frac{dX}{X} (Q^2 d^2 \xi / dX^2 + T). \quad (A1)$$

Eliminating $d^2 \Psi / dX^2$ in Eqs. (16) and (17), replacing Ψ by its constant value, and dropping terms which are small in the limit $D \sim \beta \ll 1$, Eqs. (16) - (18) become

$$\frac{d^2 \xi}{dX^2} = \frac{1}{Q^2} [(Q + iQ_*) X \Psi_0 + QX^2 \xi + (i \frac{Q_*}{D} X^2 - 1)T] \quad (A2)$$

and

$$\begin{aligned} \frac{d^2 T}{dX^2} = & Q \left(\frac{X^2}{Q^2} + \frac{2}{\Gamma_c \beta} \right) T + Q \left(S - \frac{2D}{\Gamma_c \beta} \right) \xi + \frac{D}{Q} X \Psi_0 \\ & + \frac{2iQ_*}{\Gamma_c \beta} \kappa (T - D\xi) - 2iQ^2 g \frac{d^2 \xi}{dX^2}. \end{aligned} \quad (A3)$$

The mode growth rate Q is determined by solving the inhomogeneous equations (A2) and (A3) for T and ξ , and inserting the solutions in Eq. (A1).

To solve Eqs. (A2) and (A3) we assume $g^3 \beta \gg 1$ and recall the results of Sec. III. It was found that in the limit $g^3 \beta \gg 1$ two types of localized mode were found for the homogeneous system. The first type of mode was the drift wave which had the scalings

$$X \sim g\beta^{1/2}, Q \sim Q_* \sim g\beta, D\xi \sim T.$$

Assuming these scalings in Eqs. (A2) and (A3) the dominant terms are

$$(Q + iQ_*) X \psi_0 + Q X^2 \xi + i \frac{Q_*}{D} X^2 T = 0 \quad (A4)$$

and

$$\begin{aligned} Q \left(\frac{X^2}{2} + \frac{2}{\Gamma_c \beta} \right) T + Q \left(S - \frac{2D}{\Gamma_c \beta} \right) \xi + \frac{D}{Q} X \psi_0 \\ + \frac{2iQ_*}{\Gamma_c \beta} \kappa (T - D\xi) - 2iQ^2 g \frac{d^2 \xi}{dX^2} = 0. \end{aligned} \quad (A5)$$

From Eqs. (A4) and (A5) we see $\xi \sim g^{-1} \beta^{-1/2} \psi_0$. Thus, we can estimate the contribution from the drift wave solution to the integral in Eq. (A1) to be of order $\beta^{1/2} g^{-1}$.

The second type of mode that was found in Sec. III was a highly localized density perturbation which had the scaling $X \sim g^{-1/2}$, $Q \sim Q_* \sim g\beta$, $T \sim g^3 \beta^2 \xi$. The dominant terms in Eqs. (A2) and (A3) for this mode are

$$\frac{d^2 \xi}{dX^2} = \frac{1}{2} \left[(Q + iQ_*) X \psi_0 + \left(\frac{iQ_*}{D} X^2 - 1 \right) T \right], \quad (A6)$$

and

$$\frac{d^2 T}{dX^2} = \frac{2}{\Gamma_c \beta} (Q + i\kappa Q_*) T - 2iQ^2 g \frac{d^2 \xi}{dX^2}. \quad (A7)$$

From Eqs. (A6) and (A7) we can estimate $T \sim g^{1/2} \beta \psi_0$. Consequently, the contribution to the integral in Eq. (A1) will be of order $g^{1/2} \beta \psi_0$.

On the basis of the previous estimates we conclude that in the limit $g^3 \beta \gg 1$ the integral in Eq. (A1) is dominated by the contributions coming from those values of X corresponding to the highly localized mode, i.e. $X \sim g^{-1/2}$. If one assumes $L_r \Delta' \sim g^{1/2} \beta$ then the dispersion relation is obtained by solving Eqs. (A6) and (A7) for T and ξ , and inserting the solutions in the integral in Eq. (A1).

Defining the normalized variables ϕ, Y , and a_1 , where

$$T = \frac{i(Q + iQ_*) S^{3/4} \psi_0}{4 g^{1/2}} \phi,$$

$$X = \frac{1}{2} S^{1/4} g^{-1/2} Y,$$

$$a_1 = \frac{S^{1/2}}{2g} \left(\frac{Q}{\Gamma_c \beta} + \frac{iQ_* \kappa}{\Gamma_c \beta} + ig \right).$$

Equations (A6) and (A7) can be cast in the form of an inhomogeneous Weber equation,

$$\frac{d^2 \phi}{dY^2} - \left(\frac{1}{4} Y^2 + a_1 \right) \phi = -Y. \quad (A8)$$

The integral in Eq. (A1) then becomes

$$L_r \Delta' = \frac{1}{2} S^{1/4} g^{-1/2} (Q + iQ_*) \int_{-\infty}^{\infty} dY \left(1 - \frac{1}{4} Y \phi(Y) \right). \quad (A9)$$

Equation (A8) may be solved using the Fourier transform methods discussed in Sec.

III. The resulting dispersion relation obtained from Eq. (A9) is

$$L_r \Delta' = \frac{2^{1/2} \pi S^{1/4}}{g^{1/2}} (Q + iQ_*) \frac{\Gamma(\frac{3}{4} + \frac{1}{2} a_1)}{\Gamma(\frac{1}{4} + \frac{1}{2} a_1)}. \quad (A10)$$

Equation (A10) possesses an infinite number of solutions for the growth rate Q which are associated with the poles of the gamma functions. These solutions are the odd counterparts of the localized solutions discussed in Sec. III and have a dispersion relation similar to Eq. (50). An additional solution of Eq. (A10) is present due to the factor $(Q + iQ_*)$. If $\Delta' L_r$ is small we find $Q \approx -iQ_* + \delta Q$ where

$$\delta Q = \frac{g^{1/2}}{S^{1/4}} L_r \Delta' |\Gamma(\frac{3}{4} + i\nu_1)|^{-2} (\cosh \pi \nu_1 + i \sinh \pi \nu_1)^{-1}, \quad (A11)$$

and

$$\nu_1 = \frac{S^{1/2}}{4} \left(1 + \frac{2D}{\Gamma_c \beta S} (\kappa - 1) \right).$$

Equation (A11) indicates that this mode will be unstable if $\Delta' > 0$, with marginal stability achieved at $\Delta' = 0$.

The proceeding analysis suggests that the tearing mode will be unstable for any $\Delta' > 0$. However, in deriving Eq. (A10) we have assumed $L_r \Delta' \sim g^{1/2} \beta$ and disregarded the contribution to the integral in Eq. (A1) from the drift wave region $X \sim g\beta^{1/2}$. This contribution was estimated to be of order $\beta^{1/2} g^{-1}$ and thus, Eq. (A11) breaks down for $L_r \Delta' \sim \beta^{1/2} g^{-1}$. In this case we assume $Q \approx -iQ_* + \delta Q$ where $\delta Q \sim \beta^{1/2} g^{-1/2} \ll Q_*$ and the contribution from the highly localized region scales as $\beta^{1/2} g^{-1}$. To calculate the contribution from the drift

wave region we insert $Q \sim iQ_*$ in Eqs. (A4) and (A5) and solve for ξ and T .

Defining the normalized variables Y , ϕ , and a_2 , where

$$X = (Qg)^{1/2} S^{-1/4} Y,$$

$$\xi = \frac{iD g^{1/2} \psi_0}{2 Q^{3/2} S^{1/2}} \phi,$$

and

$$a_2 = -\frac{i}{2} S^{1/2}.$$

Equations (A4) and (A5) can be rewritten,

$$\frac{d^2 \phi}{dY^2} - \left(\frac{1}{4} Y^2 + a_2 \right) \phi = -Y.$$

The contribution to the integral in Eq. (A1) becomes

$$L_r \Delta' = -\frac{i}{2} D(QgS^{1/2})^{-1/2} \int_{-\infty}^{\infty} dY \left(1 - \frac{1}{4} Y \phi(Y) \right),$$

which may be evaluated in a manner analogous to Eq. (A9)

$$L_r \Delta' = -i \frac{2^{1/2} \pi D}{Q^{1/2} g^{1/2} S^{1/4}} \frac{\Gamma(\frac{3}{4} + \frac{1}{2} a_2)}{\Gamma(\frac{1}{4} + \frac{1}{2} a_2)}. \quad (A12)$$

Combining the contributions from the drift wave and localized regions we obtain the dispersion relation,

$$L_r \Delta' = \frac{2^{1/2} \pi}{g^{1/2}} S^{1/4} \left[\delta Q \frac{\Gamma(\frac{3}{4} + \frac{1}{2} a_1)}{\Gamma(\frac{1}{4} + \frac{1}{2} a_1)} - i \frac{D}{S^{1/4} (-i Q_*)^{1/2}} \frac{\Gamma(\frac{3}{4} + \frac{1}{2} a_2)}{\Gamma(\frac{3}{4} + \frac{1}{2} a_2)} \right]. \quad (A13)$$

To assess the importance of the drift wave region we consider for simplicity the case $\kappa = 1$, $S \ll 1$ and consequently $a_1 \approx a_2 \approx 0$. The expression for the growth rate δQ reduces to

$$\delta Q = \frac{|D|^{1/2}}{(2g)^{1/2}} \exp \left(i \frac{3\pi}{4} \frac{D}{|D|} \right) + L_r \Delta' \frac{g^{1/2} \Gamma(\frac{1}{4})}{2^{1/2} \pi S^{1/4} \Gamma(\frac{3}{4})}. \quad (A14)$$

Equation (A14) indicates that a threshold value of Δ' exists below which the mode is stable, and demonstrates the stabilizing effect on the tearing mode of coupling to the drift wave.^{20,21} If we examine the definitions of g and L_r we see that the threshold is independent of η as $\eta \rightarrow 0$.

DISTRIBUTION LIST

DOE
P.O. Box 62
Oak Ridge, Tenn. 37830

UC20 Basic List (116 copies)
UC20f (192 copies)
UC20g (176 copies)

NAVAL RESEARCH LABORATORY
Washington, D.C. 20375

Code 4700 (26 copies)
Code 4790 (150 copies)

DEFENSE TECHNICAL INFORMATION CENTER
Cameron Station
5010 Duke Street
Alexandria, VA 22314 (2 copies)

EN

DAT
FILM

5

DTI